PHILOSOPHICAL TRANSACTIONS OF THE ROYAL SOCIETY A MATHEMATICAL, PHYSICAL & ENGINEERING SCIENCES

Core Level Ligand Field Splittings in Photoelectron Spectra

R. P. Gupta, J. S. Tse and G. M. Bancroft

Phil. Trans. R. Soc. Lond. A 1980 **293**, 535-569
doi: 10.1098/rsta.1980.0003

CORE LEVEL LIGAND FIELD SPLITTINGS IN PHOTOELECTRON SPECTRA

By R. P. GUPTA, J. S. TSE and G. M. BANCROFT
Centre for Chemical Physics and Department of Chemistry, University of Western Ontario, London, Ontario, Canada N6A 5B7

(*Communicated by J. M. Thomas, F.R.S. – Received* 13 *November* 1978)

CONTENTS

An electrostatic model is developed to explain the recently characterized ligand field splittings observed in the core level photoelectron spectra of main group compounds. As for the nuclear electric field gradient splittings observed by Mössbauer and n.q.r. spectroscopy, we show that the electronic splittings also originate from the asymmetric part of the ligand field. Moreover, this ligand field can be divided into the two terms analogous to those used to describe the nuclear electric field gradient splitting: the valence term, eq_v, due to the non-uniform population of the valence p, d or f orbitals on the atom M of interest; and the point charge or ligand term, eq_l, due to the non-cubic orientation of ligand point charges about M. Other 'cross' terms which are not present for the nuclear splitting are assumed to be small. We calculate the ligand term, eq_l, for the alkali and halide outer p orbitals in the alkali halides, the Tl 5d orbitals in TlCl, and the Au 4f orbitals in $AuCl_2^-$. Wherever experimental results are available, our calculations are in reasonable agreement. The splittings due to eq_v for a large number of p, d and f levels are then calculated using a 'pseudo-atomic' approach with one adjustable parameter – the excess (or deficient) valence orbital population along the z-axis, $\Delta\rho$. The two terms are combined to calculate the core level splittings in Me_2Zn, $ZnCl_2$, Me_2Cd and XeF_2. Nuclear electric field gradients in these compounds are then calculated from the electronic splittings, and shown to be generally in reasonable agreement with experiment. The importance of open shell Sternheimer shielding–antishielding parameters on both the core electronic splitting and the nuclear splitting is explored and justified.

Introduction

Since the publication of the first e.s.c.a. book (Siegbahn *et al.* 1967), there has been great chemical interest in the shifts, splittings and satellites which can be obtained from core level photo-electron spectra. Chemical shifts (Siegbahn *et al.* 1969; Carlson 1975), shake-up satellites (Siegbahn *et al.* 1969; Carlson 1975; Gelius 1974), multiplet splitting (Carlson 1975; Gelius 1974; Gupta & Sen 1974), and configuration interaction (Carlson 1974; Bancroft *et al.* 1977*f*) are now reasonably well understood and can be of considerable use to the chemist and physicist. Vibrational splittings, so common in ultraviolet photoelectron spectroscopy (Turner *et al.* 1970), have also been observed on the C 1s and N 1s core levels in such molecules as CH_4 and N_2 respectively (Gelius *et al.* 1974*b*).

A new photoelectron splitting, the so-called ligand field splitting, has been observed recently on low lying narrow core d levels in Zn (Eland 1970; Orchard & Richardson 1975; Bancroft *et al.* 1977*d*), Cd (Bancroft *et al.* 1977*c*; Bancroft *et al.* 1977*a*), Ga (Bancroft *et al.* 1977*b*), In (Bancroft *et al.* 1977*a*) and Tl (Potts & Price 1977) compounds by using narrow HeI and HeII sources. Recent absorption (Comes *et al.* 1973) and e.s.c.a. (Bancroft *et al.* 1978) spectra on the Xe 4d levels in XeF_2 and XeF_4 have also shown splitting and/or broadening which has been attributed to ligand field splittings. The splitting in all cases has been ascribed to an electrostatic ligand perturbation (rather than bonding). Following from Gupta & Sen's theoretical work (Gupta & Sen 1973*a*), we have shown (Bancroft *et al.* 1977*a*, *b*, *c*, *d*) that the asymmetric part of the crystal field (the C_2^0 or *Ds* term) is almost entirely responsible for this splitting.

Similar splittings have been observed in the photoelectron spectra of low lying p levels. In the spectra of alkali halide monomers, Price *et al.* (1974) noted an increase in the apparant spin–orbit splitting of the outer halide p spectrum, combined with a broadening or splitting of the $p_{\frac{3}{2}}$ level. These effects were attributed qualitatively to the strong electrostatic field of the alkali cation. A similar splitting of the U $6p_{\frac{3}{2}}$ level has been recently noted (Veal *et al.* 1975). It appeared that these splittings were due to the same asymmetric field which caused the d level splittings.

This splitting is of particular interest because it is caused by the same part of the ligand field that produces the electric field gradient at the nucleus (Gupta & Sen 1973*a*; Bancroft *et al.* 1977*a*). Thus, this splitting offers not only a new way of measuring the asymmetric part of the ligand field, but also a unique opportunity to look at the transmission of the ligand field through the atom to the nucleus.

At present, there are several crystal field notations which are used to characterize these splittings, and there has been some confusion in conversion factors from one notation to another. We find it useful to use the *C* parameters, but it seems important here to relate the *C* parameters to the *A* and *B* parameters which are sometimes used. Assuming that the point-charge potential satisfies Laplace's equation, it can be expanded in spherical harmonics (Abragam & Bleaney 1970), yielding

$$V = \sum_{n,m} A_n^m r^n Y_n^m(\theta, \phi). \tag{1}$$

However, the spherical harmonics can be expressed in Cartesian coordinates by using the usual transformations, to give

$$V = \sum_{n,m} A_n^m K_n^m r^n Y_n^m(x, y, z), \tag{2}$$

$$= \sum_{n,m} B_n^m r^n Y_n^m(x, y, z), \tag{2a}$$

where the coefficients B_n^m are related to A_n^m by numerical factors K_n^m as given in table 1.

A theorem due to Stevens (Stevens 1952) states that, for the purpose of evaluating the matrix elements, the $Y_n^m(x,y,z)$ may be replaced by O_n^m, which is a function of the general angular momentum operators $\hat{J}_x$, $\hat{J}_y$ and $\hat{J}_z$ (see table 16 in Abragam & Bleaney). Therefore,

$$V = \sum_{n,m} r^n B_n^m \mathscr{A}_n O_n^m(\hat{J}_x, \hat{J}_y, \hat{J}_z), \tag{3}$$

$$= \sum_{n,m} C_n^m O_n^m(\hat{J}_x, \hat{J}_y, \hat{J}_z). \tag{4}$$

TABLE 1.† VALUES OF THE COEFFICIENTS K_n^m AND $\mathscr{A}_n^m$ DEFINED BY EQUATIONS (2) AND (3)

n	m	K_n^m	$\mathscr{A}_n$(f)	$\mathscr{A}_n$(d)	$\mathscr{A}_n$(p)
2	0	$\sqrt{\frac{5}{4}}\pi^{-\frac{1}{2}}$	$-\frac{2}{45}$	$-\frac{2}{21}$	$-\frac{2}{5}$
4	0	$\frac{3}{16}\pi^{-\frac{1}{2}}$	$\frac{2}{495}$	$\frac{2}{63}$	
4	4	$\frac{3}{8}\sqrt{\frac{35}{2}}\pi^{-\frac{1}{2}}$			
6	0	$\sqrt{\frac{13}{32}}\pi^{-\frac{1}{2}}$	$-\frac{4}{3861}$		
6	6	$\frac{1}{32}\sqrt{\frac{6026}{2}}\pi^{-\frac{1}{2}}$			

† Obtained from tables 15 and 18 (in Abragam & Bleaney 1970).

The coefficients C_n^m are then related to B_n^m by a factor $r^n\mathscr{A}_n$. The values of some important $\mathscr{A}_n$ are tabulated in table 1. In previous papers, we have used the operator equivalent crystal field notation of equation (4) for fitting the observed experimental spectra. For example, for a d^9 hole state in a linear molecule (e.g. the Cd $4d^9$ state in Me_2Cd), the Hamiltonian (including spin–orbit coupling is

$$H = C_2^0[3L_z^2 - L(L+1)] + C_4^0[35L_z^2 - 30L(L+L)L_z^2 + 25L_z^2 - 6L(L+1) + 3L^2(L+1)^2] + \gamma[\tfrac{1}{2}(L_+S_- + L_-S_+) + L_zS_z], \tag{5}$$

where

$$L_\pm = L_x \pm iL_y,$$

$$S_\pm = S_x \pm iS_y.$$

The crystal field parameters C_2^0 and C_4^0 ,and the spin–orbit coupling constant, γ, have been obtained easily by fitting the five observed line positions (Bancroft *et al.* 1977*c*) with the eigenvalues of the Hamiltonian.

It is important to be able to calculate these splittings and C_2^0 values on core p, d and f levels. Molecular orbital calculations have confirmed the electrostatic nature of the splitting in XeF_2 and XeF_4 (Basch *et al.* 1971), Me_2Cd (Bancroft *et al.* 1977*c*; Sherwood & Shirley 1978) and Me_2Zn (Bancroft *et al.* 1977*d*), although the calculations generally overestimate the splitting. For example, the observed C_2^0 values for the Cd and Xe 4d splittings in Me_2Cd and XeF_2 respectively are *ca.* 80 % (Bancroft & Gupta 1978) and 65 % (Bancroft *et al.* 1978) of the *ab initio* ground state calculated values (Bancroft *et al.* 1977*c*; Basch *et al.* 1971). It is evident then that such *ab initio* calculations often do not give satisfactory agreement with experimental results in spite of the substantial computing costs involved.

The electronic excitations accompanying the photoionization process are too complex to be taken into account by minimum basis set molecular orbital calculations in relaxed hole configurations. We felt that a simpler and less expensive approach should be investigated, which can adequately explain the electronic excitations by including the electronic polarization via the Sternheimer effect (Sternheimer 1950, 1966; Gupta *et al.* 1978). The general expression of the

Sternheimer parameters as derived by Gutpa & Sen (1973*b*) can be used to write approximately the $Y_2^m(\theta, \phi)$ part of the ligand field at any site (electronic or nuclear) as (Lücken 1969):

$$eq_x = eq_v(1 - R_x) + eq_l(1 - \lambda_x), \tag{6}$$

where eq_x is the field at site x, eq_v is the field due to the valence shell electrons of the atom having the site x, eq_l is the field due to all other atoms. R_x is the atomic Sternheimer parameter and λ_x is the shielding anti-shielding parameter for the perturbations external to the atom.

We have already shown in two recent theoretical papers (Bancroft & Gupta 1978; Gupta *et al.* 1978) that both the eq_v and eq_l terms separately contribute appreciably to both the Cd 4d electronic splitting and the nuclear field gradient at the ^{111}Cd nucleus in Me_2Cd. It seemed apparent that, by using a combination of the eq_v and eq_l terms, we would be able to obtain semiquantitative estimates for both nuclear and electronic splittings, not only for Cd in Me_2Cd, but for many other elements in a variety if inorganic and organometallic compounds.

The purpose of this paper is twofold: to explain quantitatively the ligand field splittings observed to date on p and d levels by using a unified approach; and to show that this splitting should be observed in the near future on a large number of elements with high resolution photoelectron experiments. In §1, we tabulate inherently narrow (< 0.3 eV) p, d and f electronic levels in which the ligand, field splitting has been, or will be, observed. In §2, we present the underlying theory of the ligand field splitting in some detail, and justify the division of eq into the two terms in equation (6). In §3, we calculate and discuss the magnitude of the eq_l term. We begin with the simplest example – the calculation of the alkali halide spectra – considering only the electrostatic interaction of the cation or anion point charge with the anion or cation outer p levels respectively. This simple calculation yields results in quantitative agreement with experiment, and indicates how the ligand field splitting varies down the alkali metal and halogen groups in the periodic table. We then calculate the eq_l splittings for the Tl 5d orbitals in TlCl, and the Au 4f orbitals in $AuCl_2^-$. In §4, we consider the magnitude of eq_v for p, d and f levels by using the pseudo-atomic approach outlined previously (Bancroft & Gutpa 1978). The variation of eq_v from one level to another is discussed. In §5, we combine the two approaches to calculate both electronic and nuclear splittings for a number of molecules, including Me_2Zn and Me_2Cd. Then, in §6, we calculate nuclear field gradients in XeF_2, Me_2Cd, Me_2Zn and $AuCl_2^-$.

1. Narrow electronic levels

The ligand field splittings observed so far have been less than 0.5 eV. For example, the $4d_{\frac{3}{2}}$ splittings in XeF_2 and Me_2Cd are *ca.* 0.35 eV and 0.22 eV respectively (Bancroft *et al.* 1978; Bancroft *et al.* 1977*c*). Observation of these splittings obviously required high resolution spectra.

For gases, the total linewidth (Γ_t) is approximately equal to the instrumental linewidth (Γ_i) plus the natural width of the electronic level (Γ_n) (Sevier 1972; Bancroft *et al.* 1977*e*). To observe the ligand field splitting, it is thus essential to have a very small ($\leqslant 0.1$ eV) Γ_i (i.e. both narrow source linewidths (Γ_s) as are obtained from He discharge lamps and a high resolution electron analyser) *and* inherently narrow p, d and f lines.

From the instrumental point of view, it is immediately apparent that these splittings will not be observable generally by using typical laboratory X-ray sources such as Mg Kα ($\Gamma_s \approx 0.7$ eV). Present He II sources (40.8–52.2 eV) are the highest energy laboratory sources which give a narrow enough line to observe these splittings (Bancroft *et al.* 1977*a*, *b*; Potts & Price 1977). In the

near future, monochromatized synchrotron radiation will yield very narrow (< 0.1 eV) source lines up to a few hundred electronvolts (Brown *et al.* 1974), while monochromatized Al Kα radiation (Gelius *et al.* 1974*b*; Baer *et al.* 1975) may well yield linewidths in the 0.1–0.2 eV region.

Given a narrow source, the inherent linewidth of the electronic level (Γ_n) must also be very narrow. In addition, present theoretical and experimental studies indicate that the splitting decreases markedly for deep core levels (Bancroft *et al.* 1977*c*, 1978, Bancroft & Gupta 1978). In table 2, we summarize the natural widths of low lying (< 200 eV), narrow (⩽ 0.3 eV) p, d and f levels. Many of these widths are theoretical estimates, and others have not yet been estimated. However, it is apparent that a very large number of low-lying levels (mainly metal levels) have a small enough Γ_n for observation of the ligand field splitting in the gas phase. The 2p levels of Na to Cl are particularly narrow, and should prove to be particularly suitable candidates.

In the remaining sections of this paper, we will be considering the magnitude of the ligand field splittings for the elements in table 2. The inherent widths of the lines should always be kept in mind. Thus a splitting of less than 0.1 eV can be, and has been, observed for the very narrow outer d levels of Zn, Cd and Hg levels; however, such a splitting could not be seen on the d levels of Sn or Pb.

TABLE 2. NARROW, LOW BINDING ENERGY p, d AND f LEVELS OF CHEMICAL INTEREST

energy level	b.e.[a,b]/eV	width/eV	energy level	b.e.[a,b]/eV	width/eV
Na 2p	30		Cs 5p	12	
Mg 2p	50	< 0.02[c]	Ba 5p	15	
Al 2p	75	< 0.02[c,d]	La 5p	20	
Si 2p	100	< 0.02[c,d]	Ce 5p	20	
P 2p	135				
S 2p	165				
Cl 2p	200				
			Hf 4f	20	
Cl 3p	10	[e,f]	Ta 4f	25	0.053[i]
K 3p	20		W 4f	35	0.07[i]
Ca 3p	26	3×10^{-4}[g]	Re 4f	46	
Sc 3p	32		Os 4f	51	
Ti 3p	34	0.21[g]	Ir 4f	60	0.154[i]
			Pt 4f	70	
Zn 3d	16	< 0.025[h]	Au 4f	75	0.15[l], ⩽ 0.3[m]
Ga 3d	26	⩽ 0.11[h]			
Ge 3d	35	< 0.05[g]			
			Hg 5d	15	< 0.03[n]
Rb 4p	20	6×10^{-5}[i]	Tl 5d	20	⩽ 0.15[n]
Sr 4p	25		Pb 5d	25	0.32[j]
Y 4p	30	0.27[i]			
Zr 4p	35				
			Th 6p	20	[o]
Cd 4d	16	< 0.03[i]	U 6p	20	[o]
In 4d	25	⩽ 0.13[j]			
Sn 4d	30	0.14, 0.22[k]			
Xe 4d	75	*ca.* 0.1[p]			

[a] Siegbahn *et al.* (1967).
[b] Carlson (1975)
[c] Baer *et al.* (1975)
[d] Gähwiller & Brown (1970)
[e] Price *et al.* (1974)
[f] Berkowitz *et al.* (1973)
[g] McGuire (1972)
[h] Bancroft *et al.* (1977*b*)
[i] McGuire (1974)
[j] Bancroft *et al.* (1977*a*)
[k] Wertheim & Hüfner (1973)
[l] McGuire (1976)
[m] Lindau *et al.* (1975)
[n] G. M. Bancroft, D. K. Creber & J. Tse (unpublished results)
[o] Veal & Lam (1974)
[p] Svensson *et al.* (1976)

2. Theory

We begin by assuming that our molecular system can be described by a set of molecular orbitals which are linear combination of atomic orbitals (l.c.a.o.)

$$\psi_i = \sum_\mu C_{\mu i}\,\phi_\mu, \tag{7}$$

$$\sum_{\mu\nu} C^*_{\mu i}\,C_{\nu j}\,S_{\mu\nu} = \delta_{ij}, \tag{8}$$

$$S_{\mu\nu} = \langle \mu|\nu\rangle, \tag{9}$$

where ϕ_μ are atomic spin orbitals (Greek letters are used as suffixes for atomic orbitals); ψ_i are molecular wave functions (Roman letters are used as suffixes for molecular orbitals). Equation (8) results from the orthonormality of molecular orbitals. $S_{\mu\nu}$ is the overlap integral for atomic functions ϕ_μ and ϕ_ν.

The molecular wave function ψ may be expressed as an antisymmetrized product of the one electron molecular orbitals obtained by solving the Hartree–Fock equation,

$$\left[H^{\mathrm{c}} + \sum_{j=1}^{n} (2J_j - K_j)\right]\psi_i = \sum \epsilon_{ij}\,\psi_j, \tag{10}$$

or

$$F\psi_i = \sum_j \epsilon_{ij}\,\psi_j \tag{11}$$

where we have assumed that each molecular orbital is occupied by two electrons of opposite spin. H^{c} is the one-electron Hamiltonian corresponding to motion of an electron in the field of bare nuclei, and

$$J_j(1)\,\psi_i(1) = \langle j(2)|r_{12}^{-1}|j(2)\rangle\,\psi_i(1), \tag{12}$$

$$K_j(1)\,\psi_i(1) = \langle j(2)|r_{12}^{-1}|i(2)\rangle\,\psi_j(1). \tag{13}$$

The Hermitian matrix ϵ_{ij} is diagonalized to obtain unique values of $C_{\mu i}$ in equation (7) and orbital energies ϵ_i

$$F\psi_i = \epsilon_i\,\psi_i. \tag{14}$$

The problem now is to obtain approximate solutions for the perturbed molecule, when one of its atoms experiences removal of a core electron as a result of photoionization, in terms of the solutions of the unperturbed molecule. Within first order perturbation theory the desired solutions may easily be obtained as a linear combination of the appropriately symmetrized (for example, to take into account the spin–orbit interactions) molecular orbitals. Since a core electron (or hole) may be assumed to be solely confined to a particular atom A, its states can be expressed as linear combinations of certain atomic orbitals. If the core electron states are denoted by $|i^{\mathrm{c}}_{\mathrm{A}}\rangle$ we may write the matrix elements of the Fock operator F between the core electron states as

$$\langle i^{\mathrm{c}}_{\mathrm{A}}|F|j^{\mathrm{c}}_{\mathrm{A}}\rangle = \langle i^{\mathrm{c}}_{\mathrm{A}}|H^{\mathrm{c}}|j^{\mathrm{c}}_{\mathrm{A}}\rangle + 2\sum_{l=1}^{n}\sum_{\lambda\sigma} C^*_{\lambda l}\,C_{\sigma l}[\langle i^{\mathrm{c}}_{\mathrm{A}}\,\lambda|r_{12}^{-1}|\,j^{\mathrm{c}}_{\mathrm{A}}\,\sigma\rangle - \tfrac{1}{2}\langle i^{\mathrm{c}}_{\mathrm{A}}\,\lambda|r_{12}^{-1}|\,\sigma j^{\mathrm{c}}_{\mathrm{A}}\rangle]. \tag{15}$$

When the l.c.a.o. molecular orbitals are known and one is willing to perform tedious computations, equation (15) can be used to compute the matrix elements of F, and the matrix diagonalized to obtain the energies and wavefunctions of the core hole states. When this is not convenient, the various approximations of equation (15) may still yield useful solutions.

The summation over λ and σ can be divided into two components: the λ_A and σ_A summations over the atomic orbitals centred at the atomic site A, and the λ_B and σ_B summations over all the other atoms' orbitals

$$\begin{aligned}\langle i_A^c|F|j_A^c\rangle = \langle i_A^c|H^c|j_A^c\rangle + 2\sum_{l=1}^{n}\Big[&\sum_{\lambda_A\sigma_A} C^*_{\lambda_A l}C_{\sigma_A l}\{\langle i_A^c\,\lambda_A|r_{12}^{-1}|j_A^c\,\sigma_A\rangle - \tfrac{1}{2}\langle i_A^c\,\lambda_A|r_{12}^{-1}|\,\sigma_A j_A^c\rangle\}\\ &+\sum_{\lambda_B\sigma_{B'}} C^*_{\lambda_B l}C_{\sigma_{B'} l}\{\langle i_A^c\,\lambda_B|r_{12}^{-1}|j_A^c\,\sigma_{B'}\rangle - \tfrac{1}{2}\langle i_A^c\,\lambda_B|r_{12}^{-1}|\,\sigma_{B'} j_A^c\rangle\}\\ &+\sum_{\lambda_A\sigma_B} C^*_{\lambda_A l}C_{\sigma_B l}\{\langle i_A^c\,\lambda_A|r_{12}^{-1}|j_A^c\,\sigma_B\rangle - \tfrac{1}{2}\langle i_A^c\,\lambda_A|r_{12}^{-1}|\,\sigma_B j_A^c\rangle\}\\ &+\sum_{\lambda_B\sigma_A} C^*_{\lambda_B l}C_{\sigma_A l}\{\langle i_A^c\,\lambda_B|r_{12}^{-1}|j_A^c\,\sigma_A\rangle - \tfrac{1}{2}\langle i_A^c\,\lambda_B|r_{12}^{-1}|\,\sigma_A j_A^c\rangle\}\Big]. \end{aligned} \tag{16}$$

We may interpret $\langle a(1)\,b(2)\,|r_{12}^{-1}|\,c(1)\,d(2)\rangle$ as a Coulomb interaction between the charge densities $a(1)\,c(1)$ and $b(2)\,d(2)$. The first term in the square brackets contains the interactions between the charge densities involving atomic orbitals centred at A only. The first member of the second term has a Coulomb interaction between $i_A^c\,j_A^c$ and $\lambda_B\,\sigma_{B'}$, both of which involve atomic orbitals either centred only at A or only at B's. The second member of this term (exchange integral) contains a Coulomb interaction between $i_A^c\,\sigma_B$ and $\lambda_B\,j_A^c$, both of which involve atomic orbitals centred at A as well as at B's; since i_A^c and j_A^c are localized at A, we should expect the interaction to be negligibly small. The third term in equation (16) has the first member containing a Coulomb interaction between $i_A^c\,j_A^c$ and $\lambda_A\,\sigma_B$. The latter may be expected to be small except possibly in a very small region when λ_A and σ_B are involved in strong covalent bonding. The second member of the third term, involving interaction between $i_A^c\,\sigma_B$ and $\lambda_A\,j_A^c$, would be much smaller. The fourth term is similar to the third and has the same interpretation. As a first approximation, therefore, it seems reasonable to ignore the third and the fourth term in the square bracket. If one wishes to include them, it should be kept in mind that the Coulomb parts are expected to give dominant contributions. In Appendix A, we have presented a special case for a simpler understanding of equation (16).

Equation (16) may be simplified considerably for the cases having a single atomic orbital, outside the closed atomic shell, involved in bonding. Also, let us assume that $|i_A^c\rangle$ are single electron (hole) states differing only in magnetic quantum numbers

$$|\lambda_A\rangle = |\sigma_A\rangle \equiv |\alpha\rangle,\ C^*_{\lambda_A l}C_{\sigma_A l} = C_1^2;\ \ |i_A^c\rangle \equiv |nlm\rangle.$$

The first term (pseudo-atomic or atomic valence term) in the square brackets becomes

$$\pm\, 2C_1^2[\langle nlm,\alpha|r_{12}^{-1}|\,nlm',\alpha\rangle - \tfrac{1}{2}\langle nlm,\alpha|r_{12}^{-1}|\,\alpha,nlm'\rangle] \equiv \langle nlm,\alpha|\,V|\,nlm',\alpha\rangle. \tag{17}$$

The negative sign in the parentheses is valid for hole states. We recall that the factor of 2 above is due to the assumption that each orbital has two electrons of opposite spins. For diamagnetic molecules which have net spin density equal to zero, the same expression will apply with C_1^2 determining the electronic charge in the orbital as a fraction of the total charge possible in a molecular orbital, i.e. 2. It is more convenient to use C_1^2 as electronic charge. We shall therefore drop the factor of 2. Since $|nlm\rangle$ and $|\alpha\rangle$ belong to different shells, we may assume that the angular momenta coupling between them is insignificant and write

$$|nlm,\alpha\rangle = |nlm\rangle\,|\alpha\rangle. \tag{18}$$

We may arbitrarily take $|\alpha\rangle$ to be along the direction of the bond and denote it as $|NL,\,M=0\rangle$. In fact, as long as there is charge imbalance in only one orbital out of all the possible orbitals with

the same L value, we may use the formulation given here. This is because that part of the valence electron density which is equally distributed in all the orbitals with the same L will affect the energy of all possible hole states $|nlm\rangle$ $(m = 0, \pm 1, \ldots \pm l)$ by the same amount. Only the excess (or deficiency) of charge density in any of the orbitals will effect the energy of different hole states by different amounts. We may then take the z-axis to be along the orbital with excess (deficient) population, and denote the excess population as $\Delta\rho_z$.

From the expansion of the operator r_{12}^{-1} in terms of spherical harmonics $Y_l^m(\theta, \phi)$ (Slater 1960; Schläfer & Gliemann 1969),

$$r_{12}^{-1} = \sum_{k=0}^{\infty} \frac{4\pi}{2k+1} \frac{r_<^k}{r_>^{k+1}} \sum_{q=-k}^{k} (-1)^q Y_k^{-q}(\theta_1, \phi_1)\, Y_k^q(\theta_2, \phi_2), \tag{19}$$

we may write equation (17) as

$$\pm \Delta\rho_z \left[\sum_{k=0}^{\infty} a^k(lm, L0)\, F^k(nl, NL) - \tfrac{1}{2} \sum_{k=0}^{\infty} b^k(lm, L0)\, G^k(nl, NL) \right] \delta_{mm'} \equiv \langle nlm, NL0|V|nlm', NL0\rangle, \tag{20}$$

where

$$a^k(lm, L0) = \frac{4\pi}{2k+1} \sum_{q=-k}^{k} (-1)^q \langle lm|Y_k^{-q}|lm\rangle \langle L0|Y_k^q|L0\rangle,$$

$$b^k(lm, L0) = \frac{4\pi}{2k+1} \sum_{q=-k}^{k} (-1)^q \langle lm|Y_k^{-q}|L0\rangle \langle L0|Y_k^q|lm\rangle,$$

$$F^k(nl, NL) = \int_0^\infty \int_0^\infty R_{nl}^*(1)\, R_{NL}^*(2)\, R_{nl}(1)\, R_{NL}(2) \frac{r_<^k}{r_>^{k+1}} r_1^2 r_2^2 \, dr_1 \, dr_2$$

and

$$G^k(nl, NL) = \int_0^\infty \int_0^\infty R_{nl}^*(1)\, R_{NL}^*(2)\, R_{NL}(1)\, R_{nl}(2) \frac{r_<^k}{r_>^{k+1}} r_1^2 r_2^2 \, dr_1 \, dr_2. \tag{21}$$

Here, $r_<$ and $r_>$ are the lesser and greater in $r_{12} = \boldsymbol{r}_1 - \boldsymbol{r}_2$ and $|nlm> \equiv R_{nl}(r)\, Y_l^m(\theta, \phi)$. The parameters a^k and b^k are nonzero only for a limited number of k-values. For the cases of interest they have been tabulated by Slater (1960).

We want to consider all the possible combinations of core–valence interactions which give rise to splittings. Thus, we consider the interaction of p, d and f core hole states with valence p, d and f electrons. The following six cases are of practical importance:

(1) core p hole with valence p, d and f. We denote these pp′, pd and pf respectively,

(2) core d hole with valence p: dp,

(3) core f hole with valence p and d: fp, fd.

Case 1: Upon dropping the nl and NL for representing the hole and valence states respectively, we may denote the non-zero matrix elements of the Coulomb and exchange operators as

$$\langle \pm 1, 0|V|\pm 1, 0\rangle = A,$$
$$\langle 0, 0|V|0, 0\rangle = B, \tag{22}$$

where, ignoring the F^0 term which has a coefficient unity for all the cases, A and B become

1 (a) for pp′ interaction,

$$A = -\tfrac{2}{25}F^2 - \tfrac{3}{50}G^2; \quad B = \tfrac{4}{25}F^2 - \tfrac{1}{2}G^0 - \tfrac{4}{50}G^2, \tag{23}$$

1 (b) for pd interaction,

$$A = -\tfrac{2}{35}F^2 - \tfrac{1}{30}G^1 - \tfrac{18}{490}G^3; \quad B = \tfrac{4}{35}F^2 - \tfrac{4}{30}G^1 - \tfrac{27}{490}G^3, \tag{24}$$

and

1 (*c*) for pf interaction

$$A = -\tfrac{4}{75}F^2 - \tfrac{9}{350}G^2 - \tfrac{5}{189}G^4; \quad B = \tfrac{8}{75}F^2 - \tfrac{27}{350}G^2 - \tfrac{8}{189}G^4. \tag{25}$$

We have not yet included the spin–orbit interaction of the hole state. The appropriate hole states, when the spin–orbit interaction $\gamma_{nl}(\boldsymbol{l}\cdot\boldsymbol{s})$ is included, are

$$|j, m_j\rangle = \sum_{m_l m_s} \langle l, \tfrac{1}{2}, m_l, m_s | j m_j\rangle |\, l, m_l\rangle |\, s, m_s\rangle |\, L, 0\rangle. \tag{26}$$

In this expression, we have not shown the spin part of the valence orbital because we are assuming the valence spin to be zero. Using the usual notation in which an $|lm_l\rangle|s, m_s\rangle$ state is referred by the projection quantum numbers only, i.e. $|l, m_l\rangle|\, s, m_s\rangle|\, L0\rangle$ by $|m_l\, 0\rangle$ when $m_s = \frac{1}{2}$ and by $|\bar{m}_l\, 0\rangle$ when $m_s = -\frac{1}{2}$, we may write the possible j-hole states as follows

$$\left.\begin{aligned} |\tfrac{3}{2}, \tfrac{3}{2}\rangle &= |1, 0\rangle; |\tfrac{3}{2}, \tfrac{1}{2}\rangle = \sqrt{\tfrac{2}{3}}\,|0, 0\rangle + \sqrt{\tfrac{1}{3}}\,|\bar{1}, 0\rangle; \\ |\tfrac{3}{2}, -\tfrac{1}{2}\rangle &= \sqrt{\tfrac{2}{3}}\,|\bar{0}, 0\rangle + \sqrt{\tfrac{1}{3}}\,|-1, 0\rangle; |\tfrac{3}{2}, -\tfrac{3}{2}\rangle = |-\bar{1}, 0\rangle; \\ |\tfrac{1}{2}, \tfrac{1}{2}\rangle &= -\sqrt{\tfrac{1}{3}}\,|0, 0\rangle + \sqrt{\tfrac{2}{3}}\,|\bar{1}, 0\rangle; |\tfrac{1}{2}, -\tfrac{1}{2}\rangle = \sqrt{\tfrac{1}{3}}\,|\bar{0}, 0\rangle - \sqrt{\tfrac{2}{3}}\,|-1, 0\rangle. \end{aligned}\right\} \tag{27}$$

The matrix elements of the spin–orbit interaction operators are

$$\langle j, m_j|\gamma_{nl}(\boldsymbol{l}\cdot\boldsymbol{s})|j', m_{j'}\rangle = (\pm)\tfrac{1}{2}\gamma_{nl}(j(j+1) - l(l+1) - s(s+1))\,\delta_{mj\,mj'}\,\delta_{jj'}. \tag{28}$$

Again the negative sign is valid when considering a hole. Writing

$$H' = V + \gamma_{nl}(\boldsymbol{l}\cdot\boldsymbol{s}), \tag{29}$$

the non-zero matrix of H' between the j-hole states are ($\gamma_{nl} = \gamma_{np}$ for this case of p hole states)

$$\left.\begin{aligned} \langle \tfrac{3}{2}, \pm\tfrac{3}{2}|H'|\tfrac{3}{2}, \pm\tfrac{3}{2}\rangle &= A + \tfrac{1}{2}\gamma_{np}, \\ \langle \tfrac{3}{2}, \pm\tfrac{1}{2}|H'|\tfrac{3}{2}, \pm\tfrac{1}{2}\rangle &= \tfrac{1}{3}A + \tfrac{2}{3}B + \tfrac{1}{2}\gamma_{np}, \\ \langle \tfrac{3}{2}, \pm\tfrac{1}{2}|H'|\tfrac{1}{2}, \pm\tfrac{1}{2}\rangle &= \pm\sqrt{\tfrac{2}{9}}[A - B], \\ \langle \tfrac{1}{2}, \pm\tfrac{1}{2}|H'|\tfrac{1}{2}, \pm\tfrac{1}{2}\rangle &= \tfrac{2}{3}A + \tfrac{1}{3}B - \gamma_{np}. \end{aligned}\right\} \tag{30}$$

Case 2: Employing the notations developed in case 1, we may immediately write the following expressions. The non-zero matrix elements of the Coulomb and exchange operator are

$$\left.\begin{aligned} \langle \pm 2, 0|V|\pm 2, 0\rangle &= A, \\ \langle \pm 1, 0|V|\pm 1, 0\rangle &= B, \\ \langle 0, 0|V|0, 0\rangle &= C, \end{aligned}\right\} \tag{31}$$

where for the d (hole) p (valence) case

$$A = -\tfrac{4}{35}F^2 - \tfrac{15}{490}G^3; \quad B = \tfrac{2}{35}F^2 - \tfrac{3}{30}G^1 - \tfrac{24}{490}G^3$$
$$C = \tfrac{4}{35}F^2 - \tfrac{4}{30}G^1 - \tfrac{27}{490}G^3. \tag{32}$$

The j-hole states are

$$\left.\begin{aligned} |\tfrac{5}{2}, \tfrac{5}{2}\rangle &= |2, 0\rangle; |\tfrac{5}{2}, \tfrac{3}{2}\rangle = \sqrt{\tfrac{4}{5}}\,|1, 0\rangle + \sqrt{\tfrac{1}{5}}\,|,\bar{2}\,0\rangle; \\ |\tfrac{5}{2}, \tfrac{1}{2}\rangle &= \sqrt{\tfrac{2}{5}}\,|\bar{1}, 0\rangle + \sqrt{\tfrac{3}{5}}\,|0, 0\rangle; |\tfrac{5}{2}, -\tfrac{1}{2}\rangle = \sqrt{\tfrac{2}{5}}\,|-1, 0\rangle + \sqrt{\tfrac{3}{5}}\,|\bar{0}, 0\rangle; \\ |\tfrac{5}{2}, -\tfrac{3}{2}\rangle &= \sqrt{\tfrac{4}{5}}\,|-\bar{1}, 0\rangle + \sqrt{\tfrac{1}{5}}\,|-2, 0\rangle; |\tfrac{5}{2}, -\tfrac{5}{2}\rangle = |-\bar{2}, 0\rangle; \\ |\tfrac{3}{2}, \tfrac{3}{2}\rangle &= -\sqrt{\tfrac{1}{5}}\,|1, 0\rangle + \sqrt{\tfrac{4}{5}}\,|\bar{2}, 0\rangle; |\tfrac{3}{2}, \tfrac{1}{2}\rangle = \sqrt{\tfrac{3}{5}}\,|\bar{1}, 0\rangle - \sqrt{\tfrac{2}{5}}\,|0, 0\rangle; \\ |\tfrac{3}{2}, -\tfrac{1}{2}\rangle &= = \sqrt{\tfrac{3}{5}}\,|-1, 0\rangle + \sqrt{\tfrac{2}{5}}\,|\bar{0}, 0\rangle; |\tfrac{3}{2}, -\tfrac{3}{2}\rangle = \sqrt{\tfrac{1}{5}}\,|-\bar{1}, 0\rangle - \sqrt{\tfrac{4}{5}}\,|-2, 0\rangle; \end{aligned}\right\} \tag{33}$$

PHILOSOPHICAL TRANSACTIONS OF THE ROYAL SOCIETY A MATHEMATICAL, PHYSICAL & ENGINEERING SCIENCES

and the non-zero matrix elements are

$$\left.\begin{aligned}
&\langle \tfrac{5}{2}, \pm\tfrac{5}{2}|H'|\tfrac{5}{2}, \pm\tfrac{5}{2}\rangle = A+\gamma_{\mathrm{d}}; \langle \tfrac{5}{2}, \pm\tfrac{3}{2}|H'|\tfrac{5}{2}, \pm\tfrac{3}{2}\rangle = \tfrac{1}{5}A+\tfrac{4}{5}B+\gamma_{\mathrm{d}},\\
&\langle \tfrac{5}{2}, \pm\tfrac{3}{2}|H'|\tfrac{3}{2}, \pm\tfrac{3}{2}\rangle = \pm\tfrac{2}{5}[A-B]; \langle \tfrac{5}{2}, \pm\tfrac{1}{2}|H'|\tfrac{5}{2}, \pm\tfrac{1}{2}\rangle = \tfrac{2}{5}B+\tfrac{3}{5}C+\gamma_{\mathrm{d}},\\
&\langle \tfrac{5}{2}, \pm\tfrac{1}{2}|H'|\tfrac{3}{2}, \pm\tfrac{1}{2}\rangle = \pm\tfrac{\sqrt{6}}{5}[B-C]; \langle \tfrac{3}{2}, \pm\tfrac{3}{2}|H'|\tfrac{3}{2}, \pm\tfrac{3}{2}\rangle = \tfrac{4}{5}A+\tfrac{1}{5}B-\tfrac{3}{2}\gamma_{\mathrm{d}},\\
&\langle \tfrac{3}{2}, \pm\tfrac{1}{2}|H'|\tfrac{3}{2}, \pm\tfrac{1}{2}\rangle = \tfrac{3}{5}B+\tfrac{2}{5}C-\tfrac{3}{2}\gamma_{\mathrm{d}}.
\end{aligned}\right\} \tag{34}$$

Case 3: Again, from the representation developed in case 1, we may easily write the following formulae. The non-zero matrix elements of the Coulomb and exchange interaction between the f (hole) and l (valence electron) are

$$\left.\begin{aligned}
\langle \pm 3, 0|V|\pm 3, 0\rangle &= A,\\
\langle \pm 2, 0|V|\pm 2, 0\rangle &= B,\\
\langle \pm 1, 0|V|\pm 1, 0\rangle &= C,\\
\langle 0, 0|V|0, 0\rangle &= D.
\end{aligned}\right\} \tag{35}$$

where, 3 (*a*), for fp interaction,

$$\left.\begin{aligned}
A &= -\tfrac{10}{75}F^2-\tfrac{7}{378}G^4; \quad B = -\tfrac{15}{350}G^2-\tfrac{12}{378}G^4,\\
C &= \tfrac{6}{75}F^2-\tfrac{24}{350}G^2-\tfrac{15}{378}G^4; \quad D = \tfrac{8}{75}F^2-\tfrac{27}{350}G^2-\tfrac{16}{378}G^4
\end{aligned}\right\} \tag{36}$$

and, 3 (*b*), for fd interaction,

$$\left.\begin{aligned}
A &= -\tfrac{10}{105}F^2+\tfrac{18}{693}F^4-\tfrac{25}{630}G^3-\tfrac{140}{15246}G^5,\\
B &= -\tfrac{42}{693}F^4-\tfrac{315}{15246}G^5,\\
C &= \tfrac{6}{105}F^2+\tfrac{6}{693}F^4-\tfrac{6}{70}G^1-\tfrac{9}{630}G^3-\tfrac{450}{15246}G^5,\\
D &= \tfrac{8}{105}F^2+\tfrac{36}{693}F^4-\tfrac{9}{70}G^1-\tfrac{16}{630}G^3-\tfrac{500}{15246}G^5.
\end{aligned}\right\} \tag{37}$$

The appropriate wavefunctions upon including the spin–orbit coupling for the f hole are

$$\left.\begin{aligned}
|\tfrac{7}{2}, \tfrac{7}{2}\rangle &= |3, 0\rangle; |\tfrac{7}{2}, \tfrac{5}{2}\rangle = \sqrt{\tfrac{6}{7}}|2, 0\rangle+\sqrt{\tfrac{1}{7}}|\bar{3}, 0\rangle,\\
|\tfrac{7}{2}, \tfrac{3}{2}\rangle &= \sqrt{\tfrac{5}{7}}|1, 0\rangle+\sqrt{\tfrac{2}{7}}|\bar{2}, 0\rangle; |\tfrac{7}{2}, \tfrac{1}{2}\rangle = \sqrt{\tfrac{4}{7}}|0, 0\rangle+\sqrt{\tfrac{3}{7}}|\bar{1}, 0\rangle,\\
|\tfrac{7}{2}, -\tfrac{1}{2}\rangle &= \sqrt{\tfrac{4}{7}}|\bar{0}, 0\rangle+\sqrt{\tfrac{3}{7}}|-1, 0\rangle; |\tfrac{7}{2}, -\tfrac{3}{2}\rangle = \sqrt{\tfrac{5}{7}}|-\bar{1}, 0\rangle+\sqrt{\tfrac{2}{7}}|-2, 0\rangle,\\
|\tfrac{7}{2}, -\tfrac{5}{2}\rangle &= \sqrt{\tfrac{6}{7}}|-\bar{2}, 0\rangle+\sqrt{\tfrac{1}{7}}|-3, 0\rangle; |\tfrac{7}{2}, -\tfrac{7}{2}\rangle = |-\bar{3}, 0\rangle,\\
|\tfrac{5}{2}, \tfrac{5}{2}\rangle &= -\sqrt{\tfrac{1}{7}}|2, 0\rangle+\sqrt{\tfrac{6}{7}}|\bar{3}, 0\rangle; |\tfrac{5}{2}, \tfrac{3}{2}\rangle = -\sqrt{\tfrac{2}{7}}|1, 0\rangle+\sqrt{\tfrac{5}{7}}|\bar{2}, 0\rangle,\\
|\tfrac{5}{2}, \tfrac{1}{2}\rangle &= -\sqrt{\tfrac{3}{7}}|0, 0\rangle+\sqrt{\tfrac{4}{7}}|\bar{1}, 0\rangle; |\tfrac{5}{2}, -\tfrac{1}{2}\rangle = \sqrt{\tfrac{3}{7}}|\bar{0}, 0\rangle-\sqrt{\tfrac{4}{7}}|-1, 0\rangle,\\
|\tfrac{5}{2}, -\tfrac{3}{2}\rangle &= \sqrt{\tfrac{2}{7}}|-\bar{1}, 0\rangle-\sqrt{\tfrac{5}{7}}|-2, 0\rangle; |\tfrac{5}{2}, -\tfrac{5}{2}\rangle = \sqrt{\tfrac{1}{7}}|-\bar{2}, 0\rangle-\sqrt{\tfrac{6}{7}}|-3, 0\rangle,
\end{aligned}\right\} \tag{38}$$

and the non-zero matrix elements are

$$\left.\begin{aligned}
&\langle \tfrac{7}{2}, \pm\tfrac{7}{2}|H'|\tfrac{7}{2}, \pm\tfrac{7}{2}\rangle = A+\tfrac{3}{2}\gamma_{\mathrm{f}}; \langle \tfrac{7}{2}, \pm\tfrac{5}{2}|H'|\tfrac{7}{2}, \pm\tfrac{5}{2}\rangle = \tfrac{1}{7}A+\tfrac{6}{7}B+\tfrac{3}{2}\gamma_{\mathrm{f}},\\
&\langle \tfrac{7}{2}, \pm\tfrac{5}{2}|H'|\tfrac{5}{2}, \pm\tfrac{5}{2}\rangle = \pm\tfrac{\sqrt{6}}{7}[A-B]; \langle \tfrac{7}{2}, \pm\tfrac{3}{2}|H'|\tfrac{7}{2}, \pm\tfrac{3}{2}\rangle = \tfrac{2}{7}B+\tfrac{5}{7}C+\tfrac{3}{2}\gamma_{\mathrm{f}},\\
&\langle \tfrac{7}{2}, \pm\tfrac{3}{2}|H'|\tfrac{5}{2}, \pm\tfrac{3}{2}\rangle = \pm\tfrac{\sqrt{10}}{7}[B-C]; \langle \tfrac{7}{2}, \pm\tfrac{1}{2}|H'|\tfrac{7}{2}, \pm\tfrac{1}{2}\rangle = \tfrac{3}{7}C+\tfrac{4}{7}D+\tfrac{3}{2}\gamma_{\mathrm{f}},\\
&\langle \tfrac{7}{2}, \pm\tfrac{1}{2}|H'|\tfrac{5}{2}, \pm\tfrac{1}{2}\rangle = \pm\tfrac{\sqrt{12}}{7}[C-D]; \langle \tfrac{5}{2}, \pm\tfrac{5}{2}|H'|\tfrac{5}{2}, \pm\tfrac{5}{2}\rangle = \tfrac{6}{7}A+\tfrac{1}{7}B-2\gamma_{\mathrm{f}},\\
&\langle \tfrac{5}{2}, \pm\tfrac{3}{2}|H'|\tfrac{5}{2}, \pm\tfrac{3}{2}\rangle = \tfrac{5}{7}B+\tfrac{2}{7}C-2\gamma_{\mathrm{f}}; \langle \tfrac{5}{2}, \pm\tfrac{1}{2}|H'|\tfrac{5}{2}, \pm\tfrac{1}{2}\rangle = \tfrac{4}{7}C+\tfrac{3}{7}D-2\gamma_{\mathrm{f}}.
\end{aligned}\right\} \tag{39}$$

We now return to equation (16) and consider the second term in the square bracket. As we pointed out earlier, one should expect little overlap between $|i^{\mathrm{c}}_{\mathrm{A}}\rangle$ and $|\lambda_{\mathrm{B}}\rangle$. That means, using equation (19) for r_{12}^{-1} we may write

$$\langle i^{\mathrm{c}}_{\mathrm{A}}\,\lambda_{\mathrm{B}}|r_{12}^{-1}|j^{\mathrm{c}}_{\mathrm{A}}\,\sigma_{\mathrm{B}'}\rangle = \sum_{k=0}^{\infty}\frac{4\pi}{2k+1}\sum_{q=-k}^{k}(-1)^q\langle i^{\mathrm{c}}_{\mathrm{A}}|r^k Y_k^{-q}|j^{\mathrm{c}}_{\mathrm{A}}\rangle\left\langle \lambda_{\mathrm{B}}\left|\frac{1}{r^{k+1}}Y_k^q\right|\sigma_{\mathrm{B}'}\right\rangle, \tag{40}$$

PHILOSOPHICAL TRANSACTIONS OF THE ROYAL SOCIETY A MATHEMATICAL, PHYSICAL & ENGINEERING SCIENCES

and may assume the corresponding exchange term to be negligible. Again, we may take $|i_A^c\rangle \equiv |nlm\rangle$. To simplify it further we neglect the terms with $B \neq B'$, and in addition consider the cases where only one atomic orbital for each ligand participates in the bonding. Then we get

$$(\pm)\, 2 \sum_\beta C_\beta^2 \sum_{k=0}^{\infty} \frac{4}{2k+1} \langle r^k \rangle_{nl} \sum_{q=-k}^{k} (-1)^q \langle lm \,|\, Y_k^{-q} \,|\, lm' \rangle \frac{1}{R_\beta^{k+1}} Y_k^q(\theta_\beta \phi_\beta). \tag{41}$$

We have used the fact that the effect of a non-overlapping charge distribution may be taken into account by a point charge. When the charge distribution is spherically symmetrical ,we may take the charge to be located at its centre. (In fact the electronic charge distribution is polarizable. The effects of polarization may be taken into account simply by varying the effective value of the point charge.) $2C_\beta^2$ is the value of charge on ligand β expressed as a fraction of maximum number of electrons in a molecular orbital, i.e. 2. If a single electron is in a bonding orbital, then

$$C_1^2 + \sum_\beta C_\beta^2 = 1. \tag{42}$$

This equation could be useful in estimating the charge on ligands from the knowledge of charge on the metal ion.

Expression (41) in crystal field notations is expressed as (Abragam & Bleaney 1970)

$$\sum_{k=0}^{\infty} \langle r^k \rangle_{nl} \sum_{q=-k}^{k} A_k^q \langle lm \,|\, Y_k^{-q} \,|\, lm' \rangle \equiv \langle lm \,|\, V_{\text{c.f.}} \,|\, lm' \rangle, \tag{43}$$

where, upon expressing C_β^2 in terms of electron charge,

$$A_k^q = \sum_{l=1}^{n} (\pm) \frac{4\pi}{2k+1} \sum_\beta C_\beta^2 \frac{1}{R_\beta^{k+1}} Y_k^q(\theta_\beta, \phi_\beta)\, (-1)^q. \tag{44}$$

The symmetry of ligands, and the value of the electron (hole) orbital angular momentum, l, determines what terms in equation (44) are non zero. The coordinates of the ligands with respect to the central ions then yield the value of the desired A_k^q. The parameters A, B, C and D (equations 22, 31 and 35) may be redefined to include the ligand field point charge contribution. Consider for example, the p hole cases. Equation (22) may be rewritten as

$$\left.\begin{aligned} A' &= \langle \pm 1, 0 \,|\, V \,|\, \pm 1, 0 \rangle + \langle \pm 1 \,|\, V_{\text{c.f.}} \,|\, \pm 1 \rangle \\ &= A + \langle r^2 \rangle_{nl} A_2^0 \langle 11 \,|\, Y_2^0 \,|\, 11 \rangle, \\ B' &= \langle 0, 0 \,|\, V \,|\, 0, 0 \rangle + \langle 0 \,|\, V_{\text{c.f.}} \,|\, 0 \rangle \\ &= B + \langle r^2 \rangle_{nl} A_2^0 \langle 10 \,|\, Y_2^0 \,|\, 10 \rangle. \end{aligned}\right\} \tag{45}$$

The non-zero matrix elements are again given by equation (30), by replacing A and B by A' and B' respectively. However, if the terms in equation (43) with $q \neq 0$ are present, there will be some additional non-zero matrix elements determined by the condition $-m-q+m' = 0$. Referring to equation (27), we see that, for $q = \pm 2$,

$$\langle \tfrac{3}{2}, \pm\tfrac{3}{2} \,|\, H'' \,|\, \tfrac{3}{2}, \mp\tfrac{1}{2} \rangle = \sqrt{\tfrac{1}{3}} \langle r^2 \rangle_{nl} A_2^{\mp 2} \langle 1, \pm 1 \,|\, Y_2^{\pm 2} \,|\, 1, \mp 1 \rangle = \langle \tfrac{3}{2}, \pm\tfrac{1}{2} \,|\, H'' \,|\, \tfrac{3}{2}, \mp\tfrac{3}{2} \rangle, \tag{46}$$

where

$$H'' = V + V_{\text{c.f.}} + \gamma_{nl}(\boldsymbol{l} \cdot \boldsymbol{s}). \tag{47}$$

Until now we have implicitly assumed that only the electron charge density in the bonding orbital is interacting with the core vacancy, and all the other electrons are only spectators. In first order perturbation theory this is completely valid. However, Sternheimer (1950, 1966) has shown that the effect of the second order perturbation of the core electrons could be quite large.

PHILOSOPHICAL TRANSACTIONS OF THE ROYAL SOCIETY A MATHEMATICAL, PHYSICAL & ENGINEERING SCIENCES

Such a perturbation may be deemed to be produced by the multipole polarization of electronic shells. In addition, we recently showed that the second order perturbation of valence electrons is even more important (Gupta *et al.* 1978). Effectively, by employing the perturbation technique, we considerably expand the basis set of atomic wavefunctions, and relax the constraint $l \leqslant n-1$, where l is the orbital angular quantum number and n is the principal quantum number of an electron. To a good approximation, this second order perturbation may be taken into account by certain shielding–antishielding parameters, now called Sternheimer parameters, associated with the various interaction terms (Gupta *et al.* 1971).

The problem of evaluating Sternheimer parameters is nontrivial. The interactions of different symmetry have different shielding–antishielding parameters (Gupta & Sen 1973*b*, *c*). That means, for each interaction given by the Slater–Condon integrals $F^k(nl, NL)$ and $G^k(nl, NL)$, and the point-charge ligand field terms A_k^q, one will have to calculate the Sternheimer contribution. Upon including the Sternheimer effect, we may write the total interaction at the electron-vacancy nl site as (leaving aside the spin–orbit interaction),

$$-[C_1^2 \sum_k a^k(lm, L0)\,(1-R^{F,k}_{nl,NL})\,F^k(nl, NL) + \sum_k b^k(lm, L0)\,(1-R^{G,k}_{nl,NL})\,G^k(nl, NL) + \sum_k c^k(lm, lm')\,(1-\lambda^k_{nl})\,\langle r^k\rangle_{nl}\,\tfrac{1}{2}(2k+1)^{\frac{1}{2}}\,\pi^{-\frac{1}{2}}\,A_k^{m'-m}], \quad (48)$$

where R and λ are Sternheimer parameters and $c^k(lm, lm') = 2\pi^{\frac{1}{2}}(2k+1)^{-\frac{1}{2}}\langle lm|\,Y_k^{m-m'}\,|\,lm'\rangle$.

At present, one can routinely calculate $F^{F,2}_{nl,NL}$ and λ^2_{nl}, but not other Sternheimer parameters.

It is interesting that equation (48) may be quickly reduced to the nuclear site for representing the nuclear quadrupole interaction (Lücken 1969). By taking

$$\text{nuclear state} = |I, I_z = I\rangle,$$

$$F^2(\mathrm{n}, NL) = \langle r^2\rangle_{\mathrm{n}}\left\langle\frac{1}{r^3}\right\rangle_{NL}, \quad (49)$$

$$G^k(\mathrm{n}, NL) = 0, \quad (50)$$

$$a^2(II, L0) = \tfrac{4}{5}\pi\langle II\,|\,Y_2^0|\,II\rangle\langle L0\,|\,Y_2^0|\,L0\rangle, = \frac{1}{2}\frac{Q}{\langle r^2\rangle_{\mathrm{n}}}\sqrt{\tfrac{4}{5}}\pi^{\frac{1}{2}}\langle L0\,|\,Y_2^0|\,L0\rangle \quad (51)$$

$$c^2(II, II) = \sqrt{\tfrac{4}{5}}\pi^{\frac{1}{2}}\langle II\,|\,Y_2^0|\,II\rangle, = \frac{1}{2}\frac{Q}{\langle r^2\rangle_{\mathrm{n}}}, \quad (52)$$

$$R^{F,2}_{\mathrm{n},NL} \equiv R_0,$$

$$\lambda^2_{\mathrm{n}} \equiv \lambda_0,$$

we have

$$-\left[(1-R_0)\,C_1^2\,Q\left\langle\frac{1}{r^3}\right\rangle_{NL}\sqrt{\tfrac{1}{5}}\pi^{\frac{1}{2}}\langle L0\,|\,Y_2^0|\,L0\rangle + (1-\lambda_0)\,\tfrac{1}{2}Q\sqrt{\tfrac{5}{4}}\pi^{\frac{1}{2}}A_2^0\right]$$

$$= -\frac{e^2qQ}{4I(2I-1)}\langle II\,|\,3I_z^2 - I(I+1)\,|\,II\rangle$$

$$= -\tfrac{1}{4}e^2qQ, \quad (53)$$

where e^2 is implied on the left hand side. It is therefore possible to check whether the model parameter C_1^2 that gives the best fit for photoelectron spectra from the outer shell is good enough for the nuclear site and/or for inner shell photoelectron spectra.

From the foregoing formulation it becomes apparent that unless the pseudo-atomic eq_v term is negligible, it is not possible to use the experimentally derived C_2^0 parameter for comparing experimental e^2qQ measurements and the electronic-hole level splittings. When the pseudo-atomic term dominates, the more meaningful approach for the comparison of experimental data is through the parameter $\Delta\rho$. However, when both the terms are significant, such a simplistic approach becomes meaningless.

In the future, a further improvement in the calculated energy levels should be achieved by including the presently neglected cross-interaction terms in equation (16) and the corresponding Sternheimer parameters.

We have not considered F^0 and A_0^0 terms throughout on the grounds that they do not cause the splitting of the electron vacancy levels. The inclusion of these terms will automatically provide the information on the change in the centre of gravity of the energy levels under changing chemical environment (the chemical shift). It is thus also possible to calculate the chemical shift from equation (16) and we will present such calculations in a future paper. As we shall show later in this paper, certain exchange terms, G^k, also contribute to the chemical shift.

3. The point charge contribution

(a) *The alkali halides*

There have been a number of recent gas phase photoelectron studies of the halide p orbital region (binding energy of *ca.* 10 eV) of alkali halide monomers (Allen *et al.* 1973; Goodman *et al.* 1973; Berkowitz *et al.* 1973, 1974; Price *et al.* 1974). The observed spin–orbit splitting of the p levels is generally larger than the free ion value, in contrast to the much smaller value observed for covalently bonded halides such as HI (Turner *et al.* 1970), CH_3I (Cornfield *et al.* 1971), ZnI_2 (Boggess *et al.* 1973) and AgI (Vonbacho *et al.* 1976). The alkali halide spin–orbit splittings support an ionic formulation for the monomers. In addition, the apparent halide spin orbit splitting increases from CsX to NaX. Moreover, in the iodides, the $p_{\frac{3}{2}}$ peak is distinctly broader than the $p_{\frac{1}{2}}$ peak; and in NaI, the $p_{\frac{3}{2}}$ peak splits into an obvious doublet.

Theoretical models of various sophistication have been proposed to explain the above observations. Based on *ab initio* m.o. calculations, Berkowitz *et al.* (1973, 1974) were able to obtain quantitative agreement with experiment. Price *et al.* (1974) employed a simple electrostatic model to calculate the binding energies of the p levels and the apparent spin–orbit splittings. Again, good agreement with experiment was obtained but they did not consider the $^2P_{\frac{3}{2}}$ splitting. It is our intention to use the electrostatic part of the ligand field (equation (41)) due to the cation to calculate both the increase in the apparent spin orbit splitting and the $^2P_{\frac{3}{2}}$ splitting.

The point symmetry at the halide site in the alkali halides is $C_{\infty v}$ for which the only relevant crystal field parameter within a manifold of p electrons is $A_2^0\langle r^2\rangle$. The crystal potential $V_{\text{c.f.}}$ is given simply by

$$V_{\text{c.f.}} = A_2^0 r^2 Y_2^0. \tag{54}$$

Non-zero matrix elements for p electrons are given by equation (45) with

$$\begin{aligned} A &= \langle \pm 1 \,|V_{\text{c.f.}}|\, \pm 1\rangle \\ &= A_2^0\langle r^2\rangle_{np}\langle Y_1^1 \,|\, Y_2^0 \,|\, Y_1^1\rangle \\ &= -\tfrac{1}{2}\sqrt{\tfrac{1}{5}}\,\pi^{-\frac{1}{2}} A_2^0\langle r^2\rangle_{np}, \end{aligned} \tag{55}$$

$$B = \langle 0 | V_{c.f.} | 0 \rangle$$
$$= A_2^0 \langle r^2 \rangle \langle Y_1^0 | Y_2^0 | Y_1^0 \rangle$$
$$= \sqrt{\tfrac{1}{5}}\, \pi^{-\frac{1}{2}} A_2^0 \langle r^2 \rangle_{np}, \qquad (56)$$

while A_2^0 above for a unit positive charge on the alkali ions is defined as

$$A_2^0 = -\frac{4\pi}{5} \frac{Y_2^0(0,0)}{R^3}$$
$$= -\tfrac{2}{\sqrt{5}}\, \pi^{\frac{1}{2}} R^{-3} \qquad (57)$$

TABLE 3[a]. CALCULATED AND OBSERVED $(\Sigma - \Pi)$ AND $(^2\Pi_{\frac{1}{2}} - {}^2\Pi_{\frac{3}{2}})$ FOR THE OUTER HALIDE p ORBITALS OF THE ALKALI HALIDES

		observed[b]/eV			calculated/eV		
compound	R_{eq}/Å	Σ	Π	$(\Sigma - \Pi)$	$(\Sigma - \Pi)$ I[c]	II[d]	$(^2\Pi_{\frac{1}{2}} - {}^2\Pi_{\frac{3}{2}})$ I[c]
NaCl	2.78	9.80	9.34	0.46	0.466	0.583	0.067
KCl	3.29		8.92	—	0.291	0.410	0.063
RbCl	3.45		8.74	—	0.257	0.373	0.061
CsCl	3.61		8.75	—	0.230	0.309	0.059
NaBr	2.86	9.45	8.80	0.65	0.686	0.747	0.210
KBr	3.31	8.82	8.34	0.48	0.559	0.613	0.166
RbBr	3.55	8.62	8.17	0.45	0.525	0.580	0.145
CsBr	3.58	8.57	8.16	0.41	0.522	0.546	0.142
NaI	3.05	9.21	8.25	1.07	1.09	1.11	0.309
			8.03				
KI	3.51	8.66	7.68	0.98	1.00	1.03	0.226
RbI	3.64	8.48	7.51	0.97	0.991	1.01	0.207
CsI	3.94	8.40	7.48	0.92	0.971	0.991	0.169

[a] $\langle r^2 \rangle$ (a.u.) 4.050 (Cl), 5.115 (Cl^-); 5.224 (Br), 6.432 (Br^-); 7.201 (I), 8.626 (I^-) (Fischer 1978). (1 a.u. = a_0^2 where $a_0^2 = 0.5291 \times 10^{-10}$ m) γ (eV) 0.0733 (Cl), 0.3067 (Br), 0.6267 (I) (Moore 1971).
[b] Price *et al.* (1974).
[c] Calculated assuming M^+X^0.
[d] Calculated assuming M^+X^-.

The effect of this crystal field, along with the usual spin orbit splitting, is shown by the theoretical calculations presented in figure 1 (positive C_2^0) for X^- in the field of a positive cation. Several qualitative points are clear from this figure. The $^2P_{\frac{3}{2}}$ level splits into two, the $\Pi_{\frac{1}{2}}$ and $\Pi_{\frac{3}{2}}$ states. As C_2^0 (or A_2^0) increases, the separation between these two levels increases. The separation between $^2\Sigma_{\frac{1}{2}}$ and the centroid of $^2\Pi_{\frac{1}{2}}$ and $^2\Pi_{\frac{3}{2}}$ increases with an increase in C_2^0 – i.e. the apparent spin orbit splitting increases from the free ion value – as observed by Price *et al.* (1974). The theoretical calculations also show that the $^2P_{\frac{3}{2}}$ splitting depends on γ, the spin–orbit coupling parameter. For a large splitting, it is desirable to have a large γ, and a highly ionic compound.

These qualitative results are made clearer by the numerical calculations in table 3. We use theoretical values of $\langle r^2 \rangle_{np}$ and γ_{np} (footnote table 3) and assume a point unit cation charge at interatomic distances from the neutral X^0 photoionized halide (and X^- ions for comparison) derived by Price *et al.* (1974). The agreement between observed and calculated apparent spin–orbit splittings $(\Sigma - \Pi)$ for the $M^+ X^0$ species is very satisfying, and indicates, as stated by Price *et al.* (1974), that these halides can be considered to be largely ionic. The agreement with the use of the X^- wave function is not as satisfactory, indicating that the photoionized halide ion is

very similar to the uncharged ground state atom. As mentioned above, the $^2P_{\frac{3}{2}}$ splitting increases with increasing γ, and thus increases in the order Cl < Br < I. The largest calculated splitting of 0.31 eV for NaI compares favourably with the observed splitting of *ca.* 0.22 eV (Price *et al.* 1974).

The narrow inherent linewidths for the outer p levels of Cl, Br and I, taken together with the calculated splittings of more than 0.1 eV for all bromides and iodides, strongly suggests that these splittings should be observable under higher resolution conditions.

TABLE 4[a,b,c]. CALCULATED (AND OBSERVED) $(\Sigma-\Pi)$ AND $(^2\Pi_{\frac{3}{2}}-{}^2\Pi_{\frac{1}{2}})$ FOR THE OUTER ALKALI METAL p ORBITALS OF THE ALKALI HALIDES (eV)

	Cl			Br			I		
	b.e.	$(\Sigma-\Pi)$	$(^2\Pi_{\frac{3}{2}}-{}^2\Pi_{\frac{1}{2}})$	b.e.	$(\Sigma-\Pi)$	$(^2\Pi_{\frac{3}{2}}-{}^2\Pi_{\frac{1}{2}})$	b.e.	$(\Sigma-\Pi)$	$(^2\Pi_{\frac{3}{2}}-{}^2\Pi_{\frac{1}{2}})$
Na	43.11	0.19	0.09	43.40	0.18	0.07	43.90	0.18	0.05
K	26.64	0.32 (0.24)	0.20	26.91	0.31 (0.32)	0.17	27.34	0.29 (0.36)	0.12
Rb	22.40	0.95 (0.93)	0.24	22.69	0.94 (0.79)	0.20	22.98	0.93 (0.85)	0.16
Cs	18.61	1.74 (1.79)	0.29	18.61	1.74 (1.74)	0.27	19.09	1.73 (1.75)	0.21

[a] Interatomic distances data are taken from microwave spectroscopy on neutral molecules (Honig *et al.* 1954).
[b] Parameters used: $\langle r^2\rangle_{np}$ a.u.: 0.6884 (Na); 2.1645 (K); 3.1241 (Rb); 4.6019 (Cs). γ_{np}/eV: 0.1128 (Na); 0.1787 (K); 0.6100 (Rb); 1.1418 (Cs). I.P. (np)/eV: 48.92 (Na); 31.86 (K); 27.45 (Rb); 23.38 (Cs).
[c] Experimental results are given in parentheses. In case more than one peak is observed, the averaged value was used.

The outer metal p region (the Na 2p, K 3p levels etc.) of the alkali halides is also of considerable interest. Potts & Williams (1977) have recently reported the photoelectron spectra of the K, Rb and Cs metal p levels in the halides with the He II radiation, and their results provide an opportunity to test the ionic model for the metal levels. We use the bond lengths determined by microwave spectroscopy (Honig *et al.* 1954), and the γ_{np}, $\langle r^2\rangle_{np}$ and I_{np} values given in table 4 to calculate the binding energy, apparent spin–orbit splitting $(\Sigma-\Pi)$ and the $^2P_{\frac{3}{2}}$ splitting $(\Pi_{\frac{1}{2}}-\Pi_{\frac{3}{2}})$. It should be realized that the equilibrium interactomic distances determined by microwave spectroscopy are substantially shorter than the interatomic distances derived previously by Price *et al.* (1974). This is not unreasonable because the bond length in the $M^{2+}X^-$ species should be substantially shorter than that in the corresponding M^+X^0 species. In fact, the equilibrium bond distances should be upper limits for the $M^{2+}X^-$ bond length.

The calculated binding energies and spin–orbit splittings are in good agreement with the observed values (table 4). In contrast to the halide apparent spin–orbit splittings which vary with the metal (table 3), the calculated (and observed) apparent metal *n*p spin–orbit splittings do not change appreciably from one halide to another. The calculated $^2P_{\frac{3}{2}}$ splittings are in the 0.2 eV region for the K, Rb and Cs halides; and under high resolution, it should be possible to observe this splitting.

(*b*) *Thallium chloride*

We turn now to another interesting series of compounds to illustrate the effect of a point charge crystal field on core d levels and how it can be modified by Sternheimer effects. The pioneer work on the high temperature gas-phase ultraviolet photoelectron spectroscopy on Group III monohalides by Berkowitz and his coworkers suggested that in the gas phase these compounds can be regarded as ionic diatomic molecules (Berkowitz 1972). Recent He II investigations on the

thallium 5d level by Potts & Price (1977) also substantiated this description. The relevant parameters in the crystal field expansion, equation (43), for 5d levels are

$$A_2^0\langle r^2\rangle_{5d} \text{ and } A_4^0\langle r^4\rangle_{5d},$$

$$V_{c.f.} = A_2^0\langle r^2\rangle_{5d}\, Y_2^0 + A_4^0\langle r^4\rangle_{5d}\, Y_4^0. \tag{58}$$

TABLE 5[a]. CALCULATED AND OBSERVED Tl 5d SPLITTINGS FOR TlCl

approximate term	method I / eV[b]	method II / eV[c]	'observed' / eV
$^2\Sigma_{\frac{1}{2}}$	0.0	0.0	
$^2\Pi_{\frac{3}{2}}$	0.05	0.11	
$^2\Delta_{\frac{5}{2}}$	0.10	0.27	
$^2\Delta_{\frac{5}{2}} - {}^2\Sigma_{\frac{1}{2}}$	0.10	0.27	$\leqslant 0.18$
$^2\Pi_{\frac{1}{2}}$	2.24	2.25	
$^2\Delta_{\frac{3}{2}}$	2.32	2.47	
$^2\Pi_{\frac{1}{2}} - {}^2\Delta_{\frac{3}{2}}$	0.08	0.22	$\leqslant 0.12$

[a] r(Tl-Cl) = 2.48 Å (Sutton 1958, 1965), $\langle r^2\rangle_{5d} = 1.965$, $\langle r^4\rangle_{5d} = 6.446$ a.u.
[b] Pure ionic model modified by Sternheimer parameter ($\lambda_{5d} = 0.647$, see text).
[c] Pure ionic model.

Non-zero matrix elements are then given in equation (34) with

$$\begin{aligned} A &= \langle \pm 2\,|V_{c.f.}|\,\pm 2\rangle \\ &= A_2^0\langle r^2\rangle_{5d}\langle Y_2^{\pm 2}\,|\,Y_2^0|\,Y_2^{\pm 2}\rangle + A_4^0\langle r^4\rangle_{5d}\langle Y_2^{\pm 2}\,|\,Y_4^0|\,Y_2^{\pm 2}\rangle \\ &= +\tfrac{1}{7}\pi^{-\frac{1}{2}}\{-\sqrt{5}A_2^0\langle r^2\rangle_{5d} + \tfrac{1}{2}A_4^0\langle r^4\rangle_{5d}\}, \end{aligned} \tag{59}$$

$$\begin{aligned} B &= \langle \pm 1\,|V_{c.f.}|\,\pm 1\rangle \\ &= A_2^0\langle r^2\rangle_{5d}\langle Y_2^{\pm 1}\,|\,Y_2^0|\,Y_2^{\pm 1}\rangle + A_4^0\langle r^4\rangle_{5d}\langle Y_2^{\pm 1}\,|\,Y_4^0|\,Y_2^{\pm 1}\rangle \\ &= \tfrac{1}{7}\pi^{-\frac{1}{2}}\{\tfrac{\sqrt{5}}{2}A_2^0\langle r^2\rangle_{5d} - 2A_4^0\langle r^4\rangle_{5d}\}, \end{aligned} \tag{60}$$

$$\begin{aligned} C &= \langle 0\,|V_{c.f.}|\,0\rangle \\ &= A_2^0\langle r^2\rangle_{5d}\langle Y_2^0\,|\,Y_2^0|\,Y_2^0\rangle + A_4^0\langle r^4\rangle_{5d}\langle Y_2^0\,|\,Y_4^0|\,Y_2^0\rangle \\ &= \tfrac{1}{7}\pi^{-\frac{1}{2}}\{\sqrt{5}A_2^0\langle r^2\rangle_{5d} + 3A_4^0\langle r^4\rangle_{5d}\}. \end{aligned} \tag{61}$$

For a linear diatomic molecule, according to equation (44), taking a negative unit point charge,

$$A_2^0 = \sqrt{\tfrac{4}{5}}\,\pi^{\frac{1}{2}}\frac{1}{R^3}, \tag{62}$$

$$A_4^0 = \tfrac{2}{3}\pi^{\frac{1}{2}}\frac{1}{R^5}. \tag{63}$$

We use the parameters derived from H.–F. wavefunctions (footnote to table 5) and assume that the interatomic distance of the photoionized state is equal to the ground state equilibrium distance. (The ionic distance is not used here as it is very much longer than the ground state bond length, and one should expect the distance between the Tl^{2+} ion and the electron cloud on the Cl^- ion will be, if anything, shorter than the ground state interatomic distance.) We have calculated the splitting in the d levels (table 5). Although it is difficult to estimate splittings from the pubished spectra (Potts & Price 1977), there is a discrepancy between the calculated and observed vaues. The calculation overestimates the splitting between $^2\Delta_{\frac{5}{2}}$ and $^2\Sigma_{\frac{1}{2}}$ levels by *ca.* 0.1 eV

and the splitting between $^2\Pi_{\frac{1}{2}}$ and $^2\Delta_{\frac{3}{2}}$ by more than 0.1 eV. This discrepancy can be resolved if we include the Sternheimer parameter in the ionic model. The effect is due to the shielding of the 5d level by the filled 6s electrons of Tl. The Sternheimer parameter at the 5d site for the electronic configuration [Xe] $5d^{10}\ 6s^2 6p^1$ was calculated by the method of Gupta & Sen (1973 *b* *c*). If we neglect the perturbations from the 6p shell in which the radial expectation value of the perturbed 6p function $\langle u'|v|u'\rangle$ is too large compared to the interatomic distance (Gupta *et al.* 1978), we calculate $\lambda_{5d} = 0.647$. The ionic field is reduced by almost a factor of $\frac{2}{3}$. With this modified potential, calculated d splittings are in better agreement with experiment. As shown in table 5, the splitting between $^2\Delta_{\frac{5}{2}}$ and $^2\Sigma_{\frac{1}{2}}$ is 0.1 eV and the splitting between $^2\Pi_{\frac{1}{2}}$ and $^2\Delta_{\frac{3}{2}}$ is 0.08 eV.

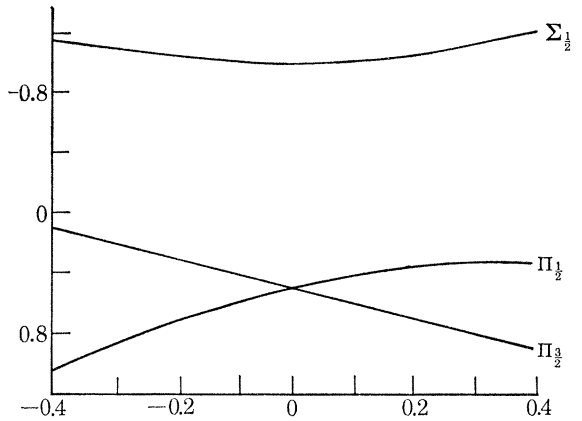

FIGURE 1. Graph of the halide p orbital energy levels in the alkali halides plotted against the magnitude of the point charge ligand field (as C_2^0 in units of γ) from the alkali cation (positive C_2^0) or anion (negative C_2^0).

(*c*) *Gold* 4f *levels*

To illustrate the effect of a crystal field on core f levels, we calculate the Au 4f splitting in the $AuCl_2^-$ ion. The large ^{197}Au nuclear splitting in $AuCl_2^-$ (Jones *et al.* 1977) indicates a large asymmetric ligand field. In this subsection, we consider just the point charge crystal field contribution, and in the next section we consider the valence contribution. Taking a linear $AuCl_2^-$ ion, there are five relevant crystal field terms, namely

$$V_{\text{c.f.}} = A_2^0 r^2 Y_2^0 + A_4^0 r^4 Y_4^0 + A_6^0 r^6 Y_6^0 + A_6^6 r^6 Y_6^6 + A_6^6 r^6 Y_6^{-6}. \tag{64}$$

With the notation developed earlier in §II, we define

$$\begin{aligned} A &= \langle \pm 3|\, V_{\text{c.f.}}\,|\pm 3\rangle \\ &= A_2^0\langle r^2\rangle_{4f}\langle Y_3^{\pm 3}\,|\,Y_2^0|\,Y_3^{\pm 3}\rangle + A_4^0\langle r^4\rangle_{4f}\langle Y_3^{\pm 3}\,|\,Y_4^0|\,Y_3^{\pm 3}\rangle \\ &\quad + A_6^0\langle r^6\rangle_{4f}\langle Y_3^{\pm 3}\,|\,Y_6^0|\,Y_3^{\pm 3} + \rangle A_6^6\langle r^6\rangle_{4f}\langle Y_3^{\pm 3}\,|\,Y_6\,|\,Y_3^{\mp 3}\rangle \end{aligned} \tag{65}$$

$$= -\frac{7\sqrt{5}}{66}\pi^{-\frac{1}{2}} A_2^0\langle r^2\rangle_{4f} - \tfrac{3}{22}\pi^{-\frac{1}{2}} A_4^0\langle r^4\rangle_{4f} - \frac{5}{66\sqrt{13}}\pi^{-\frac{1}{2}} A_6^0\langle r^6\rangle_{4f} - \sqrt{\tfrac{7}{33}}\sqrt{\tfrac{5}{13}}\pi^{-\frac{1}{2}} A_6\langle r^6\rangle_{4f}, \tag{66}$$

$$\begin{aligned} B &= \langle \pm 2\,|V_{\text{c.f.}}|\,\pm 2\rangle \\ &= A_2^0\langle r^2\rangle_{4f}\langle Y_3^{\pm 2}\,|\,Y_2^0|\,Y_3^{\pm 2}\rangle + A_4^0\langle r^4\rangle_{4f}\langle Y_3^{\pm 2}\,|\,Y_4^0|\,Y_3^{\pm 2}\rangle \\ &\quad + A_6^0\langle r^6\rangle_{4f}\langle Y_3^{\pm 2}\,|\,Y_6^0|\,Y_3^{\pm 2}\rangle + A_6^6\langle r^6\rangle_{4f}\langle Y_3^{\pm 2}\,|\,Y_6^6|\,Y_3^{\pm 2}\rangle \\ &= \tfrac{7}{22}\pi^{-\frac{1}{2}} A_4^0\langle r^4\rangle_{4f} + \tfrac{5}{11}\sqrt{\tfrac{1}{13}}\pi^{-\frac{1}{2}} A_6^0\langle r^6\rangle_{4f}, \end{aligned} \tag{67}$$

$$C = \langle \pm 1 \,|V_{\text{c.f.}}|\, \pm 1\rangle$$
$$= A_2^0\langle r^2\rangle_{4f}\langle Y_3^{\pm 1}\,|\,Y_2^0|\,Y_3^{\pm 1}\rangle + A_4^0\langle r^4\rangle_{4f}\langle Y_3^{\pm 1}\,|\,Y_4^0|\,Y_3^{\pm 1}\rangle$$
$$+ A_6^0\langle r^6\rangle_{4f}\langle Y_3^{\pm 1}\,|\,Y_6^0|\,Y_3^{\pm 1}\rangle + A_6^6\langle r^6\rangle_{4f}\langle Y_3^{\pm 1}\,|\,Y_6^6|\,Y_3^{\pm 1}\rangle$$
$$= \tfrac{2}{11}\sqrt{5}\pi^{-\frac{1}{2}} A_2^0\langle r^2\rangle_{4f} - \tfrac{1}{22}\pi^{-\frac{1}{2}} A_4^0\langle r^4\rangle_{4f} - \tfrac{25}{22\sqrt{13}}\pi^{-\frac{1}{2}} A_6^0\langle r^6\rangle_{4f}, \quad (68)$$

$$D = \langle 0\,|V_{\text{c.f.}}|\,0\rangle$$
$$= A_2^0\langle r^2\rangle_{4f}\langle Y_3^0\,|\,Y_2^0|\,Y_3^0\rangle + A_4^0\langle r^4\rangle_{4f}\langle Y_3^0\,|\,Y_4^0|\,Y_3^0\rangle$$
$$+ A_6^0\langle r^6\rangle_{4f}\langle Y_3^0\,|\,Y_6^0|\,Y_3^0\rangle + A_6^6\langle r^6\rangle_{4f}\langle Y_3^0\,|\,Y_6^6|\,Y_3^0\rangle$$
$$= \tfrac{2}{33}\sqrt{5}\pi^{-\frac{1}{2}} A_2^0\langle r^2\rangle_{4f} + \tfrac{3}{11}\pi^{-\frac{1}{2}} A_4^0\langle r^4\rangle_{4f} + \tfrac{50}{33}\sqrt{\tfrac{1}{13}}\pi^{-\frac{1}{2}} A_6^0\langle r^6\rangle_{4f}, \quad (69)$$

TABLE 6.† CALCULATED Au 4f ENERGY LEVELS IN $AuCl_2^-$/eV

approximate term	$q_{Cl} = -0.5$	$q_{Cl} = -1.0$
$^2\Delta_{\frac{1}{2}}$	0.0	0.0
$^2\Pi_{\frac{3}{2}}$	0.0007	0.0013
$^2\Phi_{\frac{5}{2}}$	0.0062	0.0124
$^2\Gamma_{\frac{7}{2}}$	0.0108	0.0217
$^2\Pi_{\frac{1}{2}}$	3.8715	3.8715
$^2\Delta_{\frac{3}{2}}$	3.8748	3.8781
$^2\Phi_{\frac{5}{2}}$	3.8816	3.8917

† r(Au-Cl) = 2.31 Å as $AuCl_2^-$ in $CsAu^{I}Au^{III}Cl_6$ (Sutton 1958, 1965). $\langle r^2\rangle_{4f} = 0.2701$ a.u. $\langle r^4\rangle = 0.1418$ a.u. $\langle r^6\rangle_{4f} = 0.1335$ a.u. $\gamma_{4f} = 1.106$ eV.

and substitute these values in equation (39) to obtain the desired non-zero matrix element. In addition to these non-zero matrix elements, two more non-zero matrix elements arise due to the Y_6^6 term in the crystal field expression

$$\langle \tfrac{7}{2}, \pm\tfrac{7}{2}\,|V_{\text{c.f.}}|\,\tfrac{7}{2}, \mp\tfrac{5}{2}\rangle = \sqrt{\tfrac{1}{7}} A_6^{\mp 6}\langle r^6\rangle_{4f}\langle Y_3^{\pm 3}\,|\,Y_6^{\pm 6}|\,Y_3^{\mp 3}\rangle$$
$$= -\sqrt{\tfrac{2}{429}}\pi^{-\frac{1}{2}} A_6^{\mp 6}\langle r^6\rangle_{4f}, \quad (70)$$

$$\langle \tfrac{7}{2}, \pm\tfrac{7}{2}\,|V_{\text{c.f.}}|\,\tfrac{5}{2}, \mp\tfrac{5}{2}\rangle = \mp\sqrt{\tfrac{6}{7}} A_6^{\mp 6}\langle r^6\rangle_{4f}\langle Y_3^{\pm 3}\,|\,Y_6^{\pm 6}|\,Y_3^{\mp 3}\rangle$$
$$= \pm 5\sqrt{\tfrac{2}{143}}\pi^{-\frac{1}{2}} A_6^{\mp 6}\langle r^6\rangle_{4f}, \quad (71)$$

where A_2^0, A_4^0, A_6^0 and A_6^6 can be evaluated from equation (44). We find, for unit negative charges on ligands,

$$A_2^0 = \sqrt{\tfrac{16}{5}}\pi^{\frac{1}{2}} R^{-3}, \quad (72)$$

$$A_4^0 = \tfrac{4}{3}\pi^{\frac{1}{2}} R^{-5}, \quad (73)$$

$$A_6^0 = \sqrt{\tfrac{16}{13}}\pi^{\frac{1}{2}} R^{-7}, \quad (74)$$

$$A_6^6 = 0. \quad (75)$$

Taking the Au^+ in $AuCl_2^-$ to be s–d hybridized with electronic configuration [Xe] $4f^{14}\,5d^9\,6s^1$, we calculate the Au 4f crystal field splitting produced by the chlorine atoms having charges from $-0.5e$ to $-1.0e$ (table 6). Parameters required for the calculation were evaluated using the HF wavefunction of the $4f^{13}$ core ionized state (footnote to table 6). For both chlorine charges, the 4f splitting is not significant, (< 0.02 eV) and certainly will not be observable. The major factor

responsible for this very small crystal field splitting is the small $\langle r^n \rangle_{4f}$ value. A point of interest emerges from this caluclation regarding the most useful notation for representing the strength of this electrostatic interaction. Since the C_n^m parameters are functions of both A_n^m and $\langle r^n \rangle$, it is more appropriate to use C_n^m to represent the crystal field interaction.

4. The pseudo-atomic (or valence) contribution

In this section, we calculate the core p, d and f splittings produced by the non-spherically symmetric valence shell of the same atom in a molecule (the first term in the square brackets of equation (16)). We have selected from table 2 a number of elements with narrow core levels, and consider all six cases described in § 2. These elements, with appropriate p, d or f core holes, are listed in table 7, along with the Hartree–Fock (Fischer 1978) atomic parameters relevant to the present work. The Hartree–Fock wavefunctions for some cases were initially calculated for the photoionized atomic state having highest possible orbital angular momentum and lowest spin. Later, we found that the wavefunctions obtained by minimizing the average energy (Slater 1960) of a given configuration gave F and G values within *ca.* 1 % of the corresponding values from the proper atomic state wavefunctions. Since it is much easier to do the computations for an 'average' (denoted ave. in Table 7) term, we decided to switch to it in the later stages of the work. For completeness, we have listed the atomic state for which the Hartree Fock calculations were done under the column 'term'.

The valence electronic configurations chosen in table 7 are usually those for hybridized states most appropriate to molecules of a given element. For example, divalent Mg, Ca, Sr, Ba, Zn, Cd, Hg and monovalent Au all form exclusively linear two-coordinate compounds in the gas phase, in which the metal atom is considered to be sp hybridized. In a number of cases (e.g. Ti, Ce, Th) the choice of electronic configuration is not so obvious. However, our very similar results for different electronic configurations of the same element (e.g. Ce^+ with the pp′ interaction) show that the values of F and G parameters do not change appreciably with choice of electronic configuration.

With the F, G and γ parameters in these tables, we have calculated the appropriate interaction matrix for the possible p, d and f hole states (equations (30), (34) and (39)). The perturbed hole states and their energies are obtained by diagonalizing the matrix. The calculation for some typical cases is graphically presented in figures 2–5, in which $\Delta\rho$ is the nonspherical part of the valence electron density (equation (20)). Thus, for the linear cases [e.g. Sr, Cd and Au], the p_z population corresponds to the nonspherical valence electron density, and $\Delta\rho$ is just this p_z population. For other cases, in which there can be either an excess or a deficiency of valence charge density along the z-axis, we plot the energy levels for both positive and negative values of $\Delta\rho$. Since $\Delta\rho$ is an adjustable parameter to fit the experimental spectrum it is possible that $\Delta\rho$ can exceed unity in the valence p orbitals of a linear molecule such as Me_2Cd. However, $\Delta\rho$ for d and f electron densities should be substantially smaller. For the p–d interaction in Zr (figure 3), we plot the energy levels with and without the exchange term.

A number of general points from table 7 and figures 2–5 should be emphasized. First, as with the nuclear quadrupole interaction, the degeneracy of the electronic states is removed, and a number of Kramers' doublets are formed. Thus, two, three and four distinct levels are formed for $J = \frac{3}{2}, \frac{5}{2}$, and $\frac{7}{2}$ states respectively. Secondly, the splittings are generally $\leqslant 0.5$ eV, as has been already observed for core p and d levels: the $4d_{\frac{3}{2}}$ splittings in Me_2Cd and XeF_2 are 0.21 eV and

PHILOSOPHICAL TRANSACTIONS OF THE ROYAL SOCIETY A MATHEMATICAL, PHYSICAL & ENGINEERING SCIENCES

TABLE 7. THE ATOMIC DESCRIPTION AND PARAMETERS RELEVANT FOR CALCULATING PSEUDO-ATOMIC SPLITTINGS

inter-action	ion	electronic configuration	$F^2(pp')$ Ryd	$G^0(pp')$ Ryd	$G^2(pp')$ Ryd	γ_p cm^{-1}	$\langle r^2\rangle$ /a.u.	$\langle r^4\rangle$/a.u.	term
pp′	Mg+	$2p^5\ 3s^1\ 3p^1$	0.0567	0.0209	0.0203	1457	0.520	—	^{2}D
	Al+	$2p^5\ 3s^1\ 3p^2$	0.0720	0.0268	0.0265	2241	0.405	—	^{1}F
	Si+	$2p^5\ 3s^1\ 3p^3$	0.0846	0.0297	0.0302	3313	0.322	—	ave.
	Si+	$2p^5\ 3s^2\ 3p^2$	0.0713	0.0243	0.0246	3304	0.324	—	ave.
	P+	$2p^5\ 3s^2\ 3p^3$	0.0995	0.0353	0.0361	4705	0.265	—	ave.
	S+	$2p^5\ 3s^2\ 3p^4$	0.1169	0.0435	0.0443	6488	0.224	—	^{2}F
	Cl+	$2p^5\ 3s^2\ 3p^5$	0.0998	0.0088	0.0178	9353	0.222	—	ave.
pp′									
	Ca+	$3p^5\ 4s^1\ 4p^1$	0.0565	0.0129	0.0154	1944	1.736	—	^{2}D
	Si+	$3p^5\ 4s^1\ 4p^2$	0.0687	0.0158	0.0191	2696	1.421	—	^{1}F
	Ti+	$3p^5\ 4s^1p^1\ 3d^2$	0.0570	0.0127	0.0150	3276	1.316	—	ave.
	Sr+	$4p^5\ 5s^1\ 5p^1$	0.0547	0.0104	0.0137	5787	2.627	—	^{2}D
	Y+	$4p^5\ 5s^1\ 5p^2$	0.0655	0.0125	0.0166	7388	2.239	—	^{1}F
	Zr+	$4p^5\ 5s^1p^1\ 4d^2$	0.0580	0.0108	0.0141	8585	2.075	—	ave.
	Ba+	$5p^5\ 6s^1\ 6p^1$	0.0516	0.0086	0.0120	9812	3.977	—	ave.
	La+	$5p^5\ 6s^1\ 6p^2$	0.0614	0.0101	0.0142	12105	3.454	—	ave.
	La+	$5p^5\ 6s^1p^1\ 5d^1$	0.0540	0.0089	0.0124	11640	3.571	—	ave.
	Ce+	$5p^5\ 6s^1p^1\ 4f^2$	0.0520	0.0087	0.0120	11587	3.636	—	ave.
	Ce+	$5p^5\ 6s^1p^1\ 5d^2$	0.0559	0.0091	0.0126	13602	3.239	—	ave.
	Ce+	$5p^5\ 6s^1p^1\ 5d\ 4f^1$	0.0542	0.0089	0.0124	12572	3.428	—	ave.
	Th+	$6p^5\ 6d^2\ 7s^1p^1$	0.0549	0.0084	0.0120	29160	4.045	—	ave.
	Th+	$6p^5\ 5f^2\ 7s^1p^1$	0.0507	0.0079	0.0112	25932	4.407	—	ave.
			F^2(pd)	G^1(pd)	G^3(pd)	γ_p	$\langle r^2\rangle$		
pd	Ti+	$3p^5\ 4s^1p^1\ 3d^2$	0.3732	0.4654	0.2824	3276	1.316	—	ave.
	Zr+	$4p^5\ 5s^1p^1\ 4d^2$	0.2702	0.3321	0.2028	8585	2.075	—	ave.
	La+	$5p^5\ 6s^1p^1\ 5d^1$	0.2086	0.2461	0.1535	11640	3.571	—	ave.
	Ce+	$5p^5\ 6s^1p^1\ 5d^2$	0.2247	0.2682	0.1674	13602	3.239	—	ave.
	Ce+	$5p^5\ 6s^1p^1\ 5d\ 4f$	0.2123	0.2510	0.1563	12572	3.428	—	ave.
	Th+	$6p^5\ 6d^2\ 7s^1p^1$	0.2000	0.2302	0.1455	29160	4.045	—	ave.

PHILOSOPHICAL TRANSACTIONS OF THE ROYAL SOCIETY A MATHEMATICAL, PHYSICAL & ENGINEERING SCIENCES

			F^2(pf)	G^2(pf)	F^4(pf)	γ_p	$\langle r^2\rangle$		term
pf	Ce^+	$5p^5\ 6s^1p^1\ 4f^2$	0.2159	0.1191	0.0910	11587	3.636	—	ave.
	Ce^+	$5p^5\ d^16s^1\ p^1\ 4f^1$	0.2190	0.1111	0.0870	12572	3.428	—	ave.
	Th^+	$6p^5\ 5f^2\ 7s^1p^1$	0.2279	0.1513	0.1118	25932	4.407	—	ave.

			F^2(dp)	G^1(dp)	G^3(dp)	γ_d	$\langle r^2\rangle$	$\langle r^4\rangle$	
dp	Zn^+	$3d^9\ 4s^1\ 4p^1$	0.0715	0.0251	0.0212	1089	0.850	1.722	^{2}F
	Ga^+	$3d^9\ 4s^1\ 4p^2$	0.0827	0.0277	0.0243	1406	0.699	1.111	^{1}G
	Ge^+	$3d^9\ 4s^1\ 4p^3$	0.0938	0.0304	0.0273	1779	0.590	0.764	^{2}H
	Cd^+	$4d^9\ 5s^1\ 5p^1$	0.0830	0.0272	0.0235	2225	1.700	5.285	^{2}F
	In^+	$4d^9\ 5s^1\ 5p^2$	0.0937	0.0293	0.0261	2719	1.466	3.816	^{1}G
	Sn^+	$4d^9\ 5s^1\ 5p^3$	0.1042	0.0313	0.0285	3268	1.288	2.881	ave.
	Hg^+	$5d^9\ 6s^1\ 6p^1$	0.0862	0.0288	0.0246	6168	2.205	8.312	ave.
	Tl^+	$5d^9\ 6s^1\ 6p^2$	0.0977	0.0310	0.0274	7253	1.960	6.313	ave.
	Pb^+	$5d^9\ 6s^1\ 6p^3$	0.1081	0.0330	0.0299	8415	1.749	4.974	ave.

			F^2(fp)	G^2(fp)	G^3(fp)	γ_f	$\langle r^2\rangle$	$\langle r^4\rangle$	
fp	Ta^+	$4f^{13}\ 6s^1p^3\ 5d^1$	0.0340	0.0080	0.0074	4702	0.425	0.384	ave.
	Ta^+	$4f^{13}\ 6s^2p^3$	0.0387	0.0093	0.0085	4711	0.422	0.376	ave.
	W^+	$4f^{13}\ 5d^2\ 6s^1p^3$	0.0343	0.0080	0.0073	5290	0.388	0.314	ave.
	Au^+	$4f^{13}\ 5d^9\ 6s^1p^1$	0.0246	0.0050	0.0047	8921	0.270	0.142	ave.

			F^2(fd)	F^4(fd)	G^1(fd)	G^3(fd)	G^5(fd)	γ_f	$\langle r^2\rangle$	$\langle r^4\rangle$	term
fd	Ta^+	$4f^{13}\ 6s^1p^3\ 5d^1$	0.1638	0.0766	0.0561	0.0517	0.0410	4702	0.425	0.384	ave.
	W^+	$4f^{13}\ 5d^2\ 6s^1p^3$	0.1719	0.0803	0.0567	0.0533	0.0425	5290	0.388	0.314	ave.
	Au^+	$4f^{13}\ 5d^9\ 6s^16p^1$	0.1954	0.0900	0.0568	0.0562	0.0458	8921	0.270	0.142	ave.
	Au^+	$4f^{13}\ 5d^9\ 6s^2$	0.1946	0.0895	0.0565	0.0559	0.0456	8921	0.270	0.142	ave.

0.35 eV respectively. High resolution spectra will obviously be necessary, to observe these splittings. Thirdly since the nondiagonal matrix elements are small in most cases (because of the large spin–orbit contribution associated with the diagonal matrix elements), we see that the energy splittings increase more or less linearly with increasing $\Delta\rho$. Fourthly, the exchange term contributes markedly to the splitting. Moreover, at least in the p–d case (figure 3), the exchange terms lead to a noticeable chemical shift effect (Shirley 1973) (figure 3*a*). It should be also emphasized here that the valence term does not give rise to a C_4^0 type splitting. Fifthly, for the 4f level, the splitting is much more sensitive to the 5d population than the 6p (figure 4). For Au^{I} and Au^{III} compounds, this splitting could well yield a sensitive way of monitoring the role of the 5d orbitals in bonding.

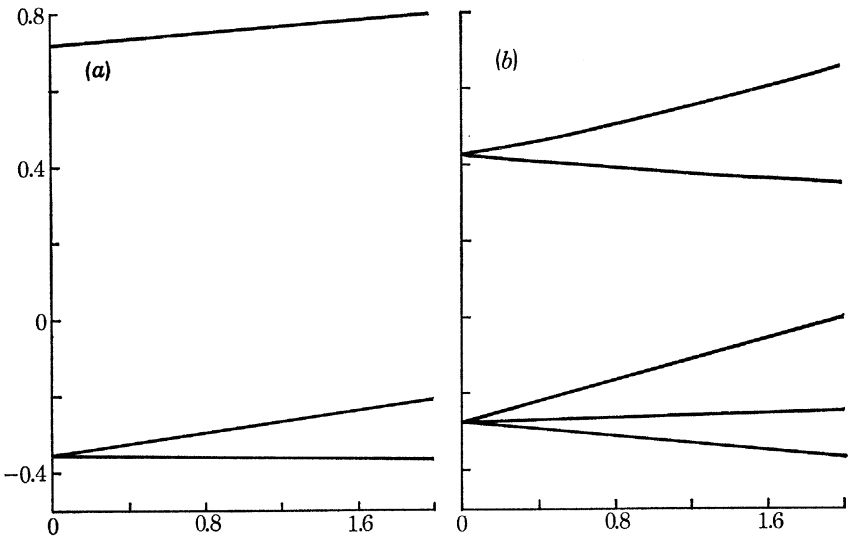

FIGURE 2. (*a*) The pp valence interaction: the 4p energies in Sr plotted against the excess $5p_z$ population. (*b*) The dp valence interaction: the 4d energies in Cd plotted against the excess $5p_z$ population.

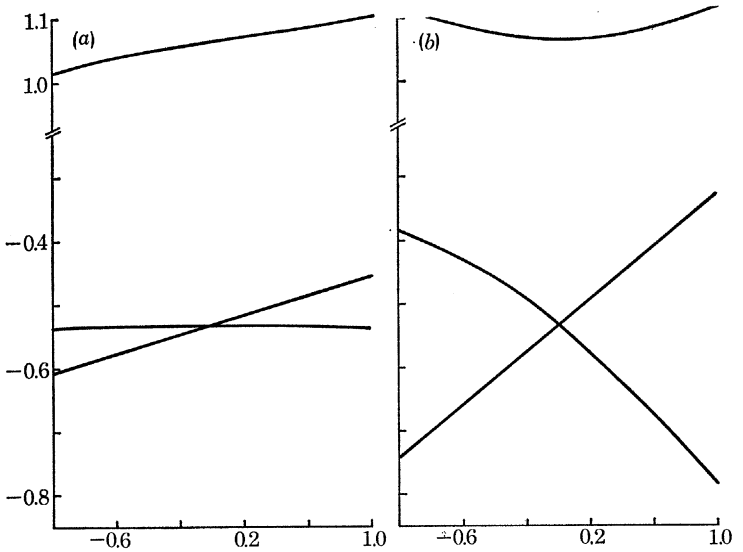

FIGURE 3. The pd valence interaction (*a*) including and (*b*) excluding the exchange terms: the 4p energies in Zr plotted against the excess (or deficiency) $4d_{z^2}$ population.

The trends in the splitting from one element to another can be semi-quantitatively estimated from table 7. For a given $\Delta\rho$, the F and G parameters (and thus the splitting) increases across a row in the Periodic Table, e.g. from Mg 2p to S 2p, or Zn 3d to Ge 3d, despite the increase in binding energy. The F and G parameters are quite constant down a group in the periodic table. Thus Mg, Ca, Sr, and Ba are all expected to give similar core $p_{\frac{3}{2}}$ splittings, as are the outer d levels of Zn, Cd and Hg.

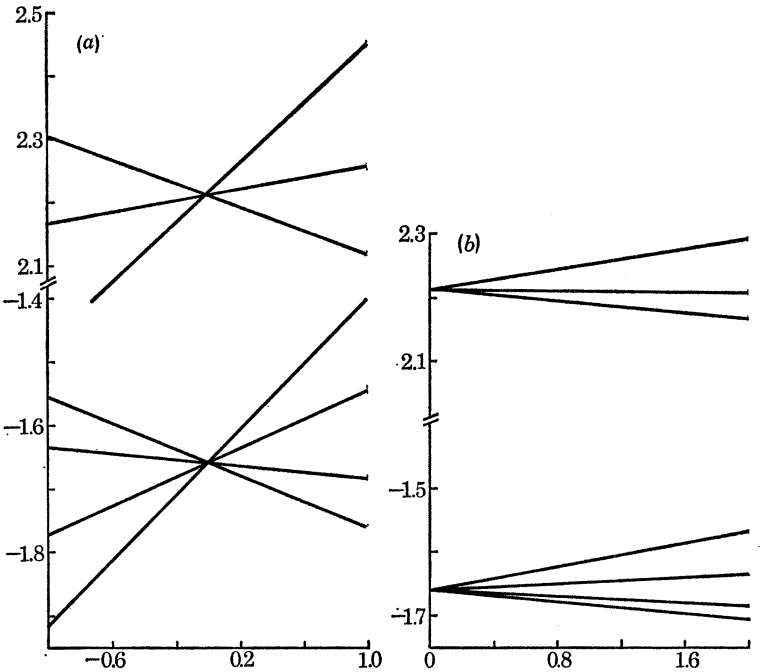

FIGURE 4. (a) The fd valence interaction and (b) the fp valence interaction: the 4f orbital energies in Au plotted against (a) the excess (or deficiency) $5d_{z^2}$ population and (b) the excess $6p_z$ population.

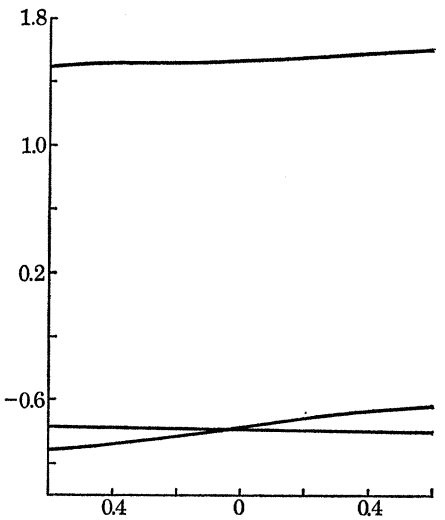

FIGURE 5. The pf valence interaction: the 5p energies in Ce plotted against the excess $5f_{z^3}$ population.

Taken together with crystal field calculations of the previous section, the results in this section show that the ligand field splitting will be observable on a large number of compounds of the elements in table 2, if very high resolution ($\leqslant 0.1$ eV) of the He lamps can be achieved at higher photon energies.

TABLE 8. OBSERVED AND CALCULATED Zn 3d ENERGIES IN Me_2Zn AND $ZnCl_2$, AND Cd 4d ENERGIES IN Me_2Cd

compound[a]	approximate term	observed[b] energies / eV	calculated energies/eV: $\Delta\rho$	valence only	$\Delta\rho$ (λ_{nd})	valence[c] + ligand	$C_4^0 \times 10^4$ eV calc. (obs.)
Me_2Zn	$^2\Sigma_{\frac{1}{2}}$	0.00		0.00		0.00	
	$^2\Pi_{\frac{3}{2}}$	0.12		0.06		0.10	
	$^2\Delta_{\frac{5}{2}}$	0.19	1.25	0.21	0.60	0.19	5.66 (7.0)
	$^2\Pi_{\frac{1}{2}}$	0.38		0.35	(0.54)	0.38	
	$^2\Delta_{\frac{3}{2}}$	0.52		0.52		0.52	
$ZnCl_2$	$^2\Sigma_{\frac{1}{2}}$	0.00		0.00		0.00	
	$^2\Pi_{\frac{3}{2}}$	*ca.* 0.12		0.05	0.70	0.06	2.00 (10.0)
	$^2\Delta_{\frac{5}{2}}$	*ca.* 0.20	1.00	0.16	(0.53)	0.16	
	$^2\Pi_{\frac{1}{2}}$	*ca.* 0.42		0.35		0.36	
	$^2\Delta_{\frac{3}{2}}$	*ca.* 0.48		0.48		0.48	
Me_2Cd	$^2\Sigma_{\frac{1}{2}}$	0.00		0.00		0.00	
	$^2\Pi_{\frac{3}{2}}$	0.13		0.07		0.13	
	$^2\Delta_{\frac{5}{2}}$	0.24	1.25	0.24	0.40	0.25	8.66 (8.0)
	$^2\Pi_{\frac{1}{2}}$	0.70		0.70	(0.49)	0.74	
	$^2\Delta_{\frac{3}{2}}$	0.90		0.90		0.91	

[a] Metal—ligand bond lengths used are: 1.83 Å in Me_2Zn (Bancroft *et al.* 1977*d*); 2.05 Å in $ZnCl_2$ (Ratner *et al.* 1977); 2.12 Å in Me_2Cd (Bakke 1972).

[b] Bancroft *et al.* 1977*c*, *d* for Me_2Zn and Me_2Cd; $ZnCl_2$ values are rough estimates from the spectra of Orchard & Richardson 1975.

[c] Charge on ligands are calculated from *ab initio* m.o. calculation: $q_C(ZnMe_2) = 0.74e$, $q_{Cl}(ZnCl_2) = 0.46e$, $q_C(CdMe_2) = 0.765e$.

5. POINT CHARGE PLUS VALENCE CONTRIBUTION

In the two previous sections, we have discussed the importance of the point charge and pseudo-atomic or valence terms to the core level splittings in ionic and covalent molecules respectively. In real molecules, we seldom find a molecule that approaches either limit; and a combination of the two terms should describe better the core level splittings. Without an *ab initio* m.o. calculation, it is often difficult to choose a reasonable charge on the ligand atoms to calculate the point charge contribution. However, even single configuration m.o. calculations often overestimate charge transfer between atoms in a molecule (Basch *et al.* 1971). To enable easy calculation of both terms with one adjustable parameter $\Delta\rho$, we assume that the charges on the nearest neighbour ligand atoms are given by the *ab initio* calculated charges. We take Me_2Zn as a specific example. It is generally recognized that the Zn–C bond in this compound has predominantly covalent character. From only the pseudo-atomic or valence term, we were able to choose a $\Delta\rho$ value of 1.25, which gave a reasonable fit to the Zn 3d photoelectron spectra (table 8). This $\Delta\rho$ value is substantially larger than the p_z orbital population of 0.43 calculated by an *ab initio* method (Bancroft *et al.* 1977*d*). Moreover, the $^2\Pi_{\frac{3}{2}}$ line position is not well reproduced: the observed

$^2\Pi_{\frac{3}{2}}$–$^2\Sigma_{\frac{1}{2}}$ splitting of 0.12 eV does not agree with the calculated value of 0.06 eV. This splitting is rather sensitive to the magnitude of C_4^0, and the pure valence model does not give rise to a C_4^0 type term. The *ab initio* calculation on Me_2Zn (Bancroft *et al.* 1977*d*) assigned a charge of -0.73e to the carbon atoms. These charges should give rise to a significant point charge contribution to *both* C_2^0 and C_4^0, and result in a smaller valence contribution and $\Delta\rho$.

Before discussing the combined calculations for Me_2Zn, we illustrate in figure 6 (*a*)–(*c*) the effects of (*a*) just the valence term, (*b*) just the ligand term, and (*c*) the combined interaction on the splitting of the Zn 3d levels as a function of $\Delta\rho$. For the ligand and combined interaction, we use the *ab initio* C charge of -0.73e to calculate the ligand term.

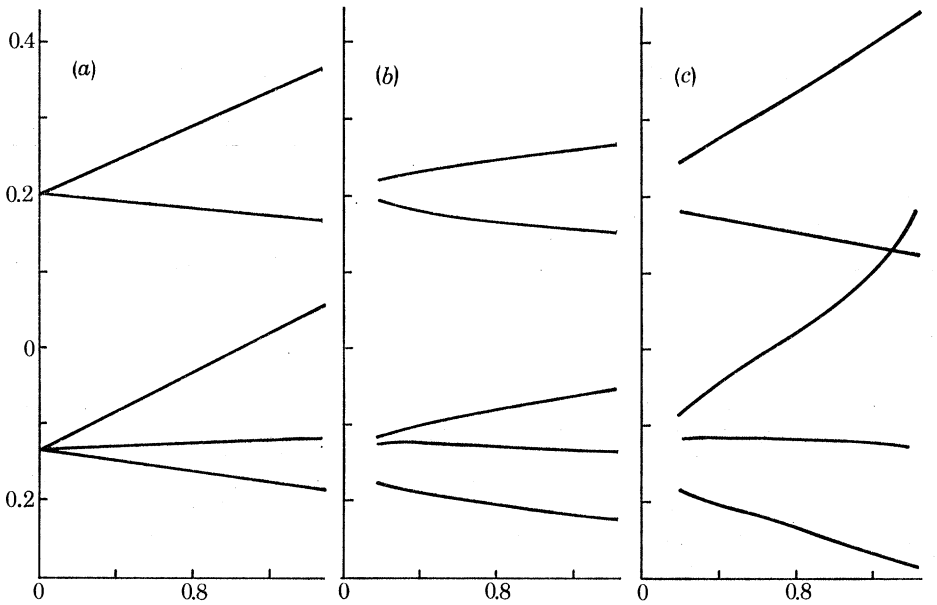

FIGURE 6. The 3d energies in Zn plotted against $\Delta\rho$, the excess population along z. (*a*) the valence only interaction; (*b*) the ligand only interaction and (*c*) the combined valence–ligand interaction.

In figure 6 (*a*), the valence-only splitting increases steadily as $\Delta\rho$ increases. The same trend was shown for the Cd 4d orbitals in figure 2 (*b*). One might expect a constant 3d splitting from the C charges (figure 6 (*b*)), but the open shell Sternheimer effect increases with $\Delta\rho$. The open shell contribution to the Sternheimer parameter is calculated by considering the valence shell closed, and multiplying this 'closed' contribution by the occupied fraction, $\Delta\rho$. For example, for p electrons

$$\lambda = (\tfrac{1}{6}a)\,\Delta\rho,$$

where a is the open shell Sternheimer contribution from six Zn 4p electrons. The combined effect of the valence and ligand terms is shown in figure 6 (*c*). A value of $\Delta\rho = 0.60$ gives the best fit to the Zn 3d photoelectron spectra of Me_2Zn. The results in table 8 show that the agreement between observed and calculated Zn 3d peak positions improves substantially when the ligand term is included with the valence term. In particular the position of the $^2\Pi_{\frac{3}{2}}$ line is significantly improved due to the inclusion of the C_4^0 term. Moreover, the calculated C_4^0 value is in very good agreement with the C_4^0 value derived from the Me_2Zn spectrum. The $\Delta\rho$ value of 0.60 is comparable to the Mulliken excess p_z population of 0.43 calculated from the pseudo-potential *ab initio* calculation

PHILOSOPHICAL TRANSACTIONS OF THE ROYAL SOCIETY A MATHEMATICAL, PHYSICAL & ENGINEERING SCIENCES

for Me_2Zn (Bancroft *et al.* 1977*d*). Similarly, the results for Me_2Cd give a $\Delta\rho$ value of 1.25 if the ligand term is neglected (table 8) and a $\Delta\rho$ value of 0.40 if it is included. Again, we observe a significant improvement in the $^2\Pi_{\frac{1}{2}}$ position when the ligand term is included. The $\Delta\rho$ value estimated is in good agreement with the *ab initio* Mulliken excess p_z population of 0.39 (Bancroft *et al.* 1977*c*). Again, the calculated C_4^0 value is in good agreement with the observed value. For $ZnCl_2$, the inclusion of the ligand contribution does not substantially improve the agreement. However, the line positions of $ZnCl_2$ are only qualitative estimates from the reported data (Orchard & Richardson 1975) and are subject to a large uncertainty. On the other hand, the *ab initio* calculated charge of $-0.46e$ on the chlorine atoms is smaller than the calculated charge on the carbon atoms in Me_2Zn.

TABLE 9. OBSERVED[a] AND CALCULATED[b] Xe $3d_{\frac{3}{2}}$ AND $4d_{\frac{3}{2}}$ SPLITTINGS IN XeF_2

				$3d_{\frac{3}{2}}$ splitting		$4d_{\frac{3}{2}}$ splitting	
model	$\Delta\rho$	λ_{3d}[c]	λ_{4d}[c]	observed[a]	calculated	observed[a]	calculated
valence only	−1.30	—	—	0.18 ± (0.06)	0.12	0.33 ± 0.04	0.33
valence plus ligand	−1.40	0.36	0.73	0.18 ± (0.06)	0.12	0.33 ± 0.04	0.33
nuclear field gradient ($\times 10^{16}$ e.s.u. cm^{-3})				8.35	5.35	8.35	5.60

[a] Bancroft *et al.* 1978.

[b] Taking r(Xe—F) = 2.00 Å (Basch *et al.* 1971). For the 3d site the following parameters were calculated (Fischer 1978) for the [Kr] $4d^{10}\,5s^2\,5p^6$ configuration: $\langle r^2\rangle_{3d} = 0.0927$ a.u., $F^2 = 0.0513$, $G^1 = 0.0129$, $G^3 = 0.01329$ (Ryd). For the 4d site, $\langle r^2\rangle_{4d} = 0.8448$ a.u. $F^2 = 0.1508$, $G^1 = 0.0422$, $G^3 = 0.0408$ (Ryd).

[c] Sternheimer parameter calculated using the atomic wavefunction of Xe with configuration [Kr] $4d^{10}\,5s^2\,5p^6$. From the configuration [Kr] $4d^{10}\,5s^2\,5p^6\,6s^1$, and neglecting the contribution of the 6s orbital, $\lambda_{3d} = 0.85$ and $\lambda_{4d} = 0.86$. These values make no appreciable difference to $\Delta\rho$ or the $d_{\frac{3}{2}}$ splittings, reflecting the small contribution of the ligand term to the splitting.

Finally, in this section it is relevant to calculate the expected splittings in both an inner and outer core d level and compare them with recent experimental results. The recent e.s.c.a. study on XeF_2 (Bancroft *et al.* 1978) showed that the Xe 3d and Xe 4d peaks (binding energies *ca.* 680 eV and *ca.* 70 eV respectively) broaden relative to the corresponding peaks in Xe gas. The 4d broadening corresponds to a $4d_{\frac{3}{2}}$ splitting of 0.33 ± 0.04 eV, while the 3d broadening corresponds to a $3d_{\frac{3}{2}}$ splitting of 0.18 ± 0.06 eV.

We consider that the electrons in the $5p_z$ orbital in Xe are withdrawn by the electronegative F atoms along the z molecular axis. Hence, the differential population, $\Delta\rho$, of the 5p orbitals is negative. The *ab initio* charge on the F atom is $-0.652e$ (Basch *et al.* 1971). We have calculated the $4d_{\frac{3}{2}}$ and $3d_{\frac{3}{2}}$ splittings (table 9) using the valence model and the combination of valence and ligand terms. Both calculations give rather good agreement with experiment. Moreover, the relative 4d and 3d splittings are reproduced rather well by the same $\Delta\rho$. The $\Delta\rho$ values obtained from both the valence and combination calculation are very similar, showing that the point charge term makes a minor contribution to the splitting in this compound. The $5p_z$ population of 0.60 derived from the $\Delta\rho$ value of -1.40, is once again very close to the *ab initio* $5p_z$ population of 0.56 in the $6\sigma_u$ orbital in XeF_2. It is also interesting to note that the calculated Xe nuclear field gradients from the 3d and 4d splittings are very similar and in qualitative agreement with the observed value (table 9).

6. Nuclear field gradients

We have shown in the previous sections of this paper that outer and inner core level electronic splittings can be reasonably well (in some cases quantitatively) reproduced with the use of only one adjustable parameter. Since the nuclear field gradient (as measured by Mössbauer and n.q.r. spectroscopy) is generated by the same asymmetric electric fields, it is, of course, possible to calculate nuclear field gradients from the $\Delta\rho$ and A_2^0 (or C_2^0) values determined from the electronic splittings. Rewriting equation (6) for the nuclear site (by now it should be clear that equation (6) is actually not valid for electronic sites),

$$eq_n = eq_v\,(1-R_n) + eq_l\,(1-\lambda_n), \tag{76}$$

and comparing this with equation (53), we obtain for valence p electrons (by taking $C_1^2 = \Delta\rho$ as before):

$$eq_v = \tfrac{4}{5}e\langle r^{-3}\rangle\,\Delta\rho, \tag{77}$$

$$eq_l = \sqrt{5}\,e\pi^{-\frac{1}{2}}A_2^0. \tag{78}$$

For a ligand-only contribution (such as expected in the alkali halides), we have calculated (and Price *et al.* 1974 have measured for NaI) eq_c at electronic sites. Then eq_n is simply given by (Gupta *et al.* 1978)

$$eq_n = eq_c(1-\lambda_n)/(1-\lambda_c), \tag{79}$$

where the subscript c refers to the core electronic site. For Na in NaCl and NaBr, the calculated Na eq_n values were in reasonable agreement with the observed values (Gupta *et al.* 1978). For example, the calculated and observed Na eq values in NaBr are 0.308 and 0.587×10^{15} e.s.u. cm^{-3} respectively. For covalent molecules such as Me_2Cd, the calculated ligand-only eq_n values are about one half of the observed value (table 10) when the open shell Sternheimer terms are included (Gupta *et al.* 1978). Although the inclusion of open-shell Sternheimer effects seems to take into account part of the valence term in an alternative way, the valence contribution, eq_v, for a covalent molecule such as Me_2Cd, must make an important contribution to eq_n. Considering only eq_v, we earlier calculated an eq_n of 0.72×10^{16} e.s.u. cm^{-3}† from the $\Delta\rho$ obtained from the Cd 4d splitting with equation (77) and assuming $(1-R_n) = 1$ (Bancroft & Gutpa 1978). In that work, we used the wrong sign for the exchange terms, but our new value for eq_n (table 10) of 1.04×10^{-16} e.s.u. cm^{-3} is still comparable and small.

Clearly, we would expect better agreement between calculated and observed values for covalent molecules if both eq_v and eq_l are considered. We have calculated eq_n for the central atoms in the molecules in table 10 from the combined model. All the Sternheimer parameters λ_n are calculated from the wavefunctions of the central metal atoms in their respective hybridized states (Zn = $3d^{10}\,4s^1\,4p^1$; Cd = $4d^{10}\,5s^1\,5p^1$; Xe = $4d^{10}\,5s^2\,5p^5\,6s^1$; Au = $5d^9\,6s^1$ and $5d^{10}\,6p^1$). The effect of the open-shell perturbation is again included by considering the valence shells closed and multiplying their contribution to the Sternheimer parameter by the occupied fraction (which in the linear molecules is $\Delta\rho$). Relative to the valence-only calculation, the present combined calculations give a somewhat poorer result (compared with experiment) for XeF_2, but a significant improvement for Me_2Cd (and probably Me_2Zn). These results show that, as for the electronic splittings in these covalent molecules, the major part of the electric field gradient is due to the eq_v term – even with the large open-shell λ_n. This is consistent with the present interpretation of

† 1 e.s.u. = 3.336×10^{-10} coulomb.

PHILOSOPHICAL TRANSACTIONS OF THE ROYAL SOCIETY A MATHEMATICAL, PHYSICAL & ENGINEERING SCIENCES

nuclear field gradients (see, for example, Bancroft & Platt 1972). Considering the simplifying assumptions made, and the great difficulty of calculating nuclear field gradients, we feel this agreement is quite satisfactory. If we consider just the dominant valence term, we obviously have to have much larger (and probably unrealistic) $\Delta\rho$ values to fit the nuclear splittings. Such unrealistic $\Delta\rho$ values have already been derived for XeF_2 (Perlow 1968), and for Sn compounds with large quadrupole splittings (Bancroft *et al.* 1974).

TABLE 10. OBSERVED AND CALCULATED NUCLEAR FIELD GRADIENTS AT SITE M

$(eq)/10^{16}$ c.s.u. cm^{-3}

MX_n	Q^a	$\langle r^{-3}\rangle_{np}{}^b$	$\lambda_n{}^c$	valence[d] calculation	ligand calculation[e] with open shell Sternheimer	present combined model	experiment[f]
XeF_2	0.41[g]	20.03	−95.96	6.83	3.00	5.60	8.35
Me_2Cd	0.50[f]	3.22	−91.22	1.04	1.26	1.38	2.61
Me_2Zn	0.18[h]	1.98	−46.76	0.64	0.91	1.34	not known
$AuCl_2^-$	0.59[h]	7.34 (15.6)[i]	—	1.90 (2.88)[i]	—	1.90 (2.88)[i]	1.78[j]

[a] barns (10^{-24} cm^2).
[b] In a.u. calculated from Fischer (1978).
[c] See text.
[d] $eq_n = \frac{4}{5}\langle r^{-3}\rangle_{np}(1-R)\,\Delta\rho_z$, where $\Delta\rho_z$ is taken from the photoelectron measurements.
[e] Derived from the photoelectron splittings on outermost closed shells (Gupta *et al.* 1978) assuming no valence contribution: $eq_n = eq_c(1-\lambda_n)/(1-\lambda_c)$.
[f] Bancroft & Sham 1977.
[g] Perlow 1968.
[h] Stevens & Stevens 1971.
[i] Values in parentheses obtained from the Au 5d wavefunction; $eq_n = \frac{4}{7}\langle r^{-3}\rangle_{nd}(1-R)\,\Delta\rho_z$.
[j] Derived from Jones *et al.* (1977).

It is interesting to calculate the nuclear field gradient in ^{197}Au and ^{67}Zn in $AuCl_2^-$ and Me_2Zn respectively. The ^{197}Au nuclear field gradient in $AuCl_2^-$ has already been measured (Jones *et al.* 1977), while it should be possible in the near future to measure ^{67}Zn nuclear electric field gradients with double resonance n.q.r. techniques (T. L. Brown, personal communication). In $AuCl_2^-$ we choose $\Delta\rho$ equal to unity, neglect the point charge contribution to the nuclear field gradient, and calculate the eq_v contribution from one 5d electron and one 6p electron from our calculated values for $\langle r^{-3}\rangle_{5d}$ and $\langle r^{-3}\rangle_{6p}$ in the Au configurations $5d^9\,6s^1$ and $5d^{10}\,6p^1$ respectively (table 10). The Au eq_v values calculated in table 10 will, of course, be upper limits because $\Delta\rho$ will be less than one. However, the calculated eq_n values are close to the observed values. It is interesting to note here that the 6p contribution to the nuclear splitting, relative to the 5d contribution, is substantially larger than that for the electronic splitting (figure 4). It should then be possible to use the two splittings to determine the extent of 5d bonding in Au compounds.

To obtain a semiquantitative estimate of $e^2q\,Q$ for ^{67}Zn in Me_2Zn, we use the ratio formula (Bancroft 1971):

$$(e^2q\,Q)_{Zn} = \frac{q_n^{Zn}}{q_n^{Cd}}\frac{Q_{Zn}}{Q_{Cd}}(e^2q\,Q)_{Cd}, \tag{80}$$

along with the calculated nuclear field gradients (eq_n) in table 10 for Me_2Cd and Me_2Zn, $Q_{^{67}Zn} = 0.18$b† (Stevens & Stevens 1971), $Q_{^{111}Cd} = 0.50$ b and $(e^2q\,Q)_{Cd}$ in $Me_2Cd = 946$ MHz (Haas &

† 1 b (barn) = 10^{-28} m^2.

Shirley 1973). We obtain an $(e^2qQ)_{^{67}Zn}$ in Me_2Zn of 332 MHz. Assuming that the Q values are reasonably accurate, this value should be accurate to 10%, and be useful in finding the resonance of this compound.

In table 11, we compare some observed C_2^0 values (and derived eq_c values) with experimental nuclear field gradients. In the covalent molecules [$Me_2Sn(BzBz)_2$, Me_2Cd and XeF_2] there is a correlation between C_2^0 and eq_n. Similarly, for the ionic species (NaCl, NaBr), there is a close correlation between the C_2^0 (and eq_c) and eq_n at the Na site. However, the results in table 11 show that the correlation does not hold if covalent molecules are compared with ionic ones. Although the C_2^0 values obtained at electronic sites might be very similar, the eq_n values may be substantially different. For example, the C_2^0 values in Me_2Cd and NaBr (Na 2p site) are very similar, but the eq_n for Cd is about five times that for Na. However, there is no indication from these results that different types of compounds will give C_2^0/eq_n ratios which differ by factors of *ca.* 25, as is the case with Me_2Cd and Cd metal if the Cd 4d metal spectrum arises from a ligand field effect Bancroft *et al.* 1976; Sherwood & Shirley 1978). Better calculations on Cd metal are now needed to distinguish between the ligand field and band broadening mechanisms in the Cd 4d metal spectrum.

TABLE 11. COMPARISON OF EXPERIMENTAL eq VALUES AT ELECTRONIC AND NUCLEAR SITES/e.s.u. cm^{-3}

compound	site	$\lvert C_2^0\rvert$eV[a]	$\lvert eq_c\rvert \times 10^{13}$	$\lvert eq_n\rvert$[c] $\times 10^{16}$
$Me_2Sn(BzBz)_2$	Sn 4d	0.036	*d*	3.39
Me_2Cd	Cd 4d	0.0225	*d*	2.61
XeF_2	Xe 4d	0.041	*d*	8.35
NaCl[b]	Na 2p	0.0326	4.467	0.677
NaBr[b]	Na 2p	0.0299	3.816	0.587
NaBr[b]	Br 4p	0.2271	3.816	2.58

[a] Bancroft *et al.* (1977*a*, *b*); Gupta *et al.* (1978).
[b] Calculated by assuming that C_2^0 is determined only by the point charge ligand contribution, and by using $C_2^0 = \frac{-\sqrt{5}}{10}\pi^{-\frac{1}{2}}\langle r^2\rangle A_2^0$ and $eq = \sqrt{5}\pi^{-\frac{1}{2}}A_2^0$.
[c] Bancroft & Sham (1977); Gupta *et al.* (1978). (1 a.u. $= 32.39\times10^{14}$ e.s.u. cm^{-3} $= 1.081\times10^{-2}$ C m^{-3})
[d] Because of the large valence contribution to the splitting, it is not realistic to derive an eq_c for these molecules.

Finally, it is interesting to consider the ratios of observed C_2^0 values more quantitatively for analogous compounds (Bancroft *et al.* 1976). For ionic compounds such as NaCl and NaBr, in which only the point charge contribution is important, we can write readily for p electrons, from equations (78) and (79), including the Sternheimer factors and remembering that $C_2^0 \propto \langle r^2\rangle A_2^0$

$$\frac{|C_2^0|_A}{|C_2^0|_B} = \frac{eq_c^A}{eq_c^B}\frac{\langle r^2\rangle_A}{\langle r^2\rangle_B}\frac{(1-\lambda_c^B)}{(1-\lambda_c^A)} \tag{81}$$

and

$$\frac{eq_n^A}{eq_n^B} = \frac{(1-\lambda_n^A)}{(1-\lambda_n^B)}\frac{(1-\lambda_c^B)}{(1-\lambda_c^A)}\frac{eq_c^A}{eq_c^B}, \tag{82}$$

where λ_n and λ_c are the Sternheimer parameters at the nuclear and electronic sites respectively. For d electrons, these formulae are applicable only if we neglect the C_4 terms. The ratios of the nuclear and electronic fields in (82) will only be similar when the ratios of the $1-\lambda$ terms are the same, and this would only be expected for the same energy level in similar molecules; for example, the Na 2p level in NaCl and BaNr. Thus $eq_c^{NaCl}/eq_c^{NaBr} = 1.17$, which compares very well indeed with the nuclear eq_n^{NaCl}/eq_n^{NaBr} ratio of 1.15.

PHILOSOPHICAL TRANSACTIONS OF THE ROYAL SOCIETY A MATHEMATICAL, PHYSICAL & ENGINEERING SCIENCES

We now want to investigate the ratio of observed C_2^0 values (equation (5)) for two covalent compounds, such as Me_2Cd and Me_2Zn, in which the valence term is dominant. In a previous publication (Bancroft *et al.* 1976), it was noted that the observed C_2^0 ratio would be proportional to the ratio of the F^2 parameters,

$$\frac{|C_2^0|_A}{|C_2^0|_B} \propto \frac{F_A^2}{F_B^2}. \tag{83}$$

For the above to be true, we have to neglect the spin–orbit coupling of the core hole and the point charge term. In addition, C_2^0 is dependent only on F^2 if the exchange terms can be neglected.

To look at the nature of the proportionality constant, we study a specific example (the 'dp' interation) in more detail, neglecting the point charge term. Under the interaction of the d hole with a p valence electron, the $nd_{\frac{3}{2}}$ level will split into two levels. The energy separation is simply the difference in the eigenvalues between the $|\frac{3}{2}, \pm\frac{3}{2}\rangle$ and $|\frac{3}{2}, \pm\frac{1}{2}\rangle$ states. Following equation (34),

$$\begin{aligned}\Delta E_{nd_{\frac{3}{2}}} &= \langle \tfrac{3}{2}, \pm\tfrac{3}{2}|H'|\tfrac{3}{2}, \pm\tfrac{3}{2}\rangle - \langle \tfrac{3}{2}, \pm\tfrac{1}{2}|H'|\tfrac{3}{2}, \pm\tfrac{1}{2}\rangle, \\ &= \tfrac{1}{5}\Delta\rho(4A - 2B - 2C)\end{aligned} \tag{84}$$

while A and B are given in equation (32), so that

$$\Delta E_{nd_{\frac{3}{2}}} = -\tfrac{2}{5}\Delta\rho(\tfrac{14}{35}F^2 - \tfrac{7}{30}G^1 + \tfrac{21}{490}G^3). \tag{85}$$

If we employ the Hamiltonian defined in equation (5) and again neglect the C_4^0 and the spin–orbit coupling terms, we obtain the energy splitting between the $|\frac{3}{2}, \pm\frac{3}{2}\rangle$ and $|\frac{3}{2}, \pm\frac{1}{2}\rangle$ states as a function of C_2^0

$$\Delta E_{nd_{\frac{3}{2}}} = 6C_2^0. \tag{86}$$

We can then compare the energy splitting of the core d level under the interaction of p valence electrons for two molecules A and B by writing

$$\Delta E_{nd_{\frac{3}{2}}}/\Delta E_{nd_{\frac{3}{2}}} = \frac{C_2^0(A)}{C_2^0(B)} = \frac{-\Delta\rho_A(\frac{14}{35}F_A^2 - \frac{7}{30}G_A^1 + \frac{21}{490}G_A^3)}{-\Delta\rho_B(\frac{14}{35}F_B^2 - \frac{7}{30}G_B^1 + \frac{21}{490}G_B^3)}. \tag{87}$$

Inspecting table 7, we see that G^1 and G^3 are usually considerably smaller than F^2. We neglect them for practical purposes. Including the Sternheimer parameter for F^2, (R_{np}), we rewrite equation (87) as

$$\Delta E_{nd_{\frac{3}{2}}}^A/\Delta E_{nd_{\frac{3}{2}}}^B = \frac{C_2^0(A)}{C_2^0(B)} = \frac{\Delta\rho_A}{\Delta\rho_B}\frac{(1-R_{np}^A)}{(1-R_{np}^B)}\frac{F_A^2}{F_B^2}. \tag{88}$$

The proportionality constant $\Delta\rho_A/\Delta\rho_B$ is different from that, q_A/q_B, proposed earlier (Bancroft *et al.* 1976), but equation (77) shows that these two ratios are indeed related.

Let us consider two examples of the use of equation (88). For compounds of the same element (e.g. $ZnCl_2$ and Me_2Zn), the ratio of the observed Zn 3d C_2^0 values is just the ratios of $\Delta\rho$ obtained by fitting the spectra as in § 5. For instance, the ratio of $\Delta\rho$ obtained by the valence-only calculation for Me_2Zn and $ZnCl_2$ is 1.25, whereas the ratio of observed C_2^0 values is 1.54. The ratios of the *ab initio* calculated Zn $4p_z$ population (Rätner *et al.* 1977; Bancroft, *et al.* 1977*d*) is 1.40 – rather close to the observed C_2^0 ratio.

For molecules with different central metal atoms but very similar bonding configurations (for instance, in Me_2Zn and Me_2Cd) we assume that the Sternheimer parameters are identical, neglect the C_4^0 term, and take the F^2 values in table 7 and the $\Delta\rho$ values obtained from fitting the experimental splitting pattern from simply the valence only calculation. We calculate $\Delta E_{3d_{\frac{3}{2}}}^{Zn}$/

$\Delta E^{\mathrm{Cd}}_{4\mathrm{d}\frac{3}{2}} = 0.85$ (0.86, if we neglect all exchange integrals). These values are comparable to the experimental $\Delta\rho$ ratio of 0.74. It is also not surprising that we obtained good agreement between the ratio of the experimental C^{Q}_2 and eq_{n} values for Me_2Cd and $Me_2Sn(BzBz)_2$ (Bancroft *et al.* 1976). The major contribution to the field gradient comes from the axial methyl groups in both cases.

Equation (88) should, of course, be used with caution. Although we have neglected the ionic contribution in the above discussion of Me_2Zn, $ZnCl_2$ and Me_2Cd, the results in § 5 and table 8 showed that the ionic contribution is substantial. For core holes of higher azimuthal quantum numbers (e.g. d and f), the ratio formula can only be regarded as an approximate formula. Nonvanishing higher harmonics in the potential expansion will contribute to the total field gradient. Nevertheless, it still remains a very useful relation in estimating the electric field gradient at core and electronic sites, provided that data for similar compounds are available. One should obviously resort to using equations (48) and (53), retaining all the relevant terms, if a better correlation is to be established between the origin of the electronic and nuclear level splittings.

Conclusions

By using a fairly simple electrostatic model involving just one adjustable parameter, $\Delta\rho$, we have obtained at least semiquantitative agreement with the recently reported core level ligand field splittings in the alkali halides and Group II B and Group III halides and alkyls. Moreover, we have shown that this splitting will be observable on a large number of core levels when high resolution spectra can be obtained above 50 eV photon energies.

Although the present model should form the theoretical basis for this new photoelectron splitting, more theoretical work is obviously needed. For example, calculations of the 'cross' terms in equation (16) must be performed to confirm our assumption; and a more rigorous method is required to assign point charges to calculate eq_1 in covalent compounds. Calculations are required to show whether relaxation effects contribute significantly to the splittings. More work is also required to calculate the Sternheimer parameters in equation (48). This paper, along with the experimental nuclear and electronic splittings, should provide considerable incentive for these, and other, theoretical developments.

Appendix

To clarify the theoretical derivation, let us consider the Zn 3d core level splitting in a hypothetical molecule, ZnH_2.

The total molecular wavefunction for the photoionized state (removal of an electron in the $\sigma 1_{\mathrm{g}}$ orbital) can be expressed as the antisymmetrized product of the molecular orbitals,

$$\Phi_{\mathrm{i}} = \hat{A}|\Phi_{\mathrm{c}}\, 1\sigma_{\mathrm{g}}\, 1\pi_{\mathrm{g}}^4\, 1\delta_{\mathrm{g}}^2\, 2\sigma_{\mathrm{g}}^2\, 1\sigma_{\mathrm{u}}^2\rangle, \tag{A 1}$$

where Φ_{c} represents the product of the core molecular orbitals; $1\sigma_{\mathrm{g}}$, $1\pi_{\mathrm{g}}$ and $1\delta_{\mathrm{g}}$ are the majority Zn 3d orbitals; and $2\sigma_{\mathrm{g}}$ and $1\sigma_{\mathrm{u}}$ are the Zn–H bonding orbitals. The orbital energies can be obtained by solving the Hartree–Fock equation [equations (10), (16)] and we obtain the orbital energy of the photoionized $1\sigma_{\mathrm{g}}$ orbital, $\epsilon_{1\sigma_{\mathrm{g}}}$,

$$\epsilon_{1\sigma_{\mathrm{g}}} = \epsilon^{\mathrm{n}}_{1\sigma_{\mathrm{g}}} + \sum_{i}^{\mathrm{core}} (2J-K)_{1\sigma_{\mathrm{g}}\, i} + \tfrac{1}{2}(2J-K)_{1\sigma_{\mathrm{g}}\, 2\sigma_{\mathrm{g}}} + \tfrac{1}{2}(2J-K)_{1\sigma_{\mathrm{g}}\, 1\sigma_{\mathrm{u}}} + (2J-K)_{1\sigma\ 1\pi_{\mathrm{g}}} + (2J-K)_{1\sigma_{\mathrm{g}}\, 1\delta_{\mathrm{g}}}, \tag{A 2}$$

where J and K are calculated from equations (12) and (13) respectively, and $\sum_{i}^{\text{core}}$ are the interactions between the core molecular orbitals and the $1\sigma_g$ orbital. The term $\epsilon^{n}_{1\sigma_g}$ is the energy of the $1\sigma_g$ electron moving under the potential of a bare nucleus.

We can construct l.c.a.o.–m.o. for the valence $2\sigma_g$ and $1\sigma_u$ molecular orbitals ($|nlm_l\rangle$),

$$2\sigma_g = C_1 |4, 0, 0\rangle_{Zn} + C_2 |\psi^+\rangle, \tag{A 3}$$

$$1\sigma_u = C_3 |4, 1, 0\rangle_{Zn} + C_4 |\psi^-\rangle, \tag{A 4}$$

where

$$|\psi^+\rangle = |0\rangle_{H_a} + |0\rangle_{H_b}, \tag{A 5}$$

$$|\psi^-\rangle = |0\rangle_{H_a} - |0\rangle_{H_b}, \tag{A 6}$$

$|4, 0, 0\rangle_{Zn}$ and $|4, 1, 0\rangle_{Zn}$ are the 4s and $4p_z$ orbitals of the Zn atom respectively and $|0\rangle_{H_i}$ is the 1s orbital of the ith hydrogen atom.

We assume that the $1\sigma_g$, $1\pi_g$ and $1\delta_g$ orbital of ZnH_2 are primary 3d orbitals of Zn, i.e.,

$$\left.\begin{aligned} 1\sigma_g &\approx |3, 2, 0\rangle_{Zn}, \\ 1\pi_g &\approx |3, 2, \pm 1\rangle_{Zn}, \\ 1\delta_g &\approx |3, 2, \pm 2\rangle_{Zn}. \end{aligned}\right\} \tag{A 7}$$

Consider a typical Coulomb integral, $J_{1\sigma_g\, 2\sigma_g}$ (dropping out the subscript for convenience),

$$\begin{aligned} J_{1\sigma_g\, 2\sigma_g} &= \langle 3, 2, 0| \left(C_1\langle 4, 0, 0| + C_2\langle\psi^+|\right) r_{12}^{-1} \left(C_1| 4, 0, 0\rangle + C_2|\psi^+\rangle\right)| 3, 2, 0\rangle \\ &= C_1^* C_1 \langle 3, 2, 0|\langle 4, 0, 0| r_{12}^{-1} |4, 0, 0\rangle| 3, 2, 0\rangle + C_2^* C_2 \langle 3, 2, 0|\langle\psi^+| r_{12}^{-1} |\psi^+\rangle| 3, 2, 0\rangle \\ &\quad + C_1^* C_2 \langle 3, 2, 0|\langle 4, 0, 0| r_{12}^{-1} |\psi^+\rangle |3, 2, 0\rangle + C_2^* C_1 \langle 3, 2, 0|\langle\psi^+| r_{12}^{-1} |4, 0, 0\rangle| 3, 2, 0\rangle. \end{aligned}$$

Similarly, (A 8)

$$\begin{aligned} J_{1\sigma_g\, 1\sigma_u} &= C_3^* C_3 \langle 3, 2, 0|\langle 4, 1, 0| r_{12}^{-1}| 4, 1, 0\rangle|3, 2, 0\rangle + C_4^* C_4 \langle 3, 2, 0|\langle\psi^-| r_{12}^{-1}| \psi^-\rangle| 3, 2, 0\rangle \\ &\quad + C_3^* C_4 \langle 3, 2, 0|\langle 4, 1, 0| r_{12}^{-1}| \psi^-\rangle| 3, 2, 0\rangle + C_4^* C_3 \langle 3, 2, 0|\langle\psi^-| r_{12}^{-1}| 4, 1, 0\rangle|3, 2, 0\rangle \end{aligned}$$

and (A 9)

$$\begin{aligned} K_{1\sigma_g\, 1\sigma_u} &= \langle 3, 2, 0| \left(C_3\langle 4, 1, 0| + C_4\langle\psi^-|\right) r_{12}^{-1}|3, 2, 0\rangle| \left(C_3|4, 1, 0\rangle + C_4|\psi^-\rangle\right) \\ &= C_3^* C_3 \langle 3, 2, 0|\langle 4, 1, 0| r_{12}^{-1}|3, 2, 0\rangle| 4, 1, 0\rangle + C_4^* C_4 \langle 3, 2, 0|\langle\psi^-| r_{12}^{-1}| 4, 1, 0\rangle|\psi^-\rangle \\ &\quad + C_3^* C_4 \langle 3, 2, 0|\langle 4, 1, 0| r_{12}^{-1}|3, 2, 0\rangle|\psi^-\rangle + C_4^* C_3 \langle 3, 2, 0|\langle\psi^-| r_{12}^{-1}|3, 2, 0\rangle |4, 1, 0\rangle. \end{aligned} \tag{A 10}$$

Since we are only interested in the relative energy differences between $1\sigma_g$, $1\pi_g$ and $1\delta_g$ orbitals, we can assume the core contributions to the Coulomb and exchange terms will be cancelled off. To a further approximation, as explained in § 2, we also neglect all the two centre integrals. Then, we obtain the relative orbital energy for $1\sigma_g$ orbital, $\epsilon^{rel}_{1\sigma_g}$

$$\epsilon^{rel}_{1\sigma_g} = C_3^* C_3 \{\langle 3, 2, 0|\langle 4, 1, 0| r_{12}^{-1} | 4, 1, 0\rangle |3, 2, 0\rangle - \tfrac{1}{2}\langle 3, 2, 0|\langle 4, 1, 0| r_{12}^{-1}| 3, 2, 0\rangle |4, 1, 0\rangle\}.$$

Making use of the r_{12}^{-1} expansion in equation (19), and using the notation defined in equation (2), we write

$$|n, l, m\rangle = R_{nl}| l, m\rangle,$$

where R_{nl} is the radial wavefunction

$$\epsilon^{\mathrm{rel}}_{1\sigma_g} = C_3^* C_3 \sum_{k=0}^{\infty} \frac{4\pi}{2k+1} \Big\{ \langle 3,2,0| \langle 4,1,0| \frac{r_<^k}{r_>^{k+1}} \sum_{q=-k}^{k} (-1)^q Y_k^{-q} Y_k^q |4,1,0\rangle |3,2,0\rangle$$
$$-\frac{1}{2} \langle 3,2,0| \langle 4,1,0| \frac{r_<^k}{r_>^{k+1}} \sum_{q=-k}^{k} (-1)^q Y_k^{-q} Y_k^q |3,2,0\rangle |4,1,0\rangle \Big\}, \quad \text{(A 11)}$$

$$= C_3^* C_3 \sum_{k=0}^{\infty} \frac{4\pi}{2k+1} \Big\{ \sum_{q=-k}^{k} (-1)^q \langle 2,0| Y_k^{-q} |2,0\rangle \langle 1,0| Y_k^q |1,0\rangle \langle R_{32}| \langle R_{41}| \frac{r_<^k}{r_>^{k+1}} |R_{41}\rangle |R_{32}\rangle$$
$$-\frac{1}{2} \sum_{q=-k}^{k} (-1)^q \langle 2,0| Y_k^{-q} |1,0\rangle \langle 1,0| Y_k^q |2,0\rangle \langle R_{32}| \langle R_{41}| \frac{r_<^k}{r_>^{k+1}} |R_{32}\rangle |R_{41}\rangle \Big\}, \quad \text{(A 12)}$$

$$= C_3^* C_3 \sum_{k=0}^{\infty} \{ a^k(2,0;1,0)\, F^k(3,2;4,1) - \tfrac{1}{2} b^k(2,0;1,0)\, G^k(3,2;4,1) \}. \quad \text{(A 13)}$$

Writing $\Delta\rho = C_3^* C_3$, we get

$$\epsilon^{\mathrm{rel}}_{1\sigma_g} = \Delta\rho \sum_{k=0}^{\infty} \{ a^k(2,0;1,0)\, F^k(3,2;4,1) - \tfrac{1}{2} b^k(2,0;1,0)\, G^k(3,2;4,1) \}, \quad \text{(A 14)}$$

which is identical in form to equation (20). For this hypothetical molecule, the p_z orbital of Zn only contributes to the bonding in the $1\sigma_u$ m.o., hence the charge density of the Zn p_z orbital is

$$\mathrm{pop}\,(p_z) = \sum_{j\,\mathrm{m.o.}} C_{ij}^* C_{ij}$$
$$= C_3^* C_3. \quad \text{(A 15)}$$

Therefore, the differential charge along the z axis ($\Delta\rho$) equals $C_3^* C_3$ exactly.

Next, let us consider the two-centre terms ($T(1,2)$) that we have neglected:

$$T(1,2) = C_2^* C_2 \langle 3,2,0| \langle \psi^+| r_{12}^{-1} |\psi^+\rangle |3,2,0\rangle + C_4^* C_4 \langle 3,2,0| \langle \psi^-| r_{12}^{-1} |\psi^-\rangle |3,2,0\rangle. \quad \text{(A 16)}$$

With Mulliken's approximation (Dewar 1969), equation A 16 becomes

$$T(1,2) \approx C_2^* C_2 S_{2,0} R_{12}^{-1} S_{\psi^+} + C_4^* C_4 S_{2,0} R_{12}^{-1} S_{\psi^-}, \quad \text{(A 17)}$$

where $S_i = \langle i|i\rangle$ is the overlap integral, and R_{12} is the interatomic distance. When $|\psi^+\rangle$, $|\psi^-\rangle$, $|2,0\rangle$ are properly normalized wavefunctions, i.e. $S_i = 1$, we get

$$T(1,2) = (C_2^* C_2 + C_4^* C_4)\, R_{12}^{-1}, \quad \text{(A 18)}$$
$$= (q_{\mathrm{H_a}} + q_{\mathrm{H_b}})/R_{12}, \quad \text{(A 19)}$$

which is the ligand point charge contribution. In general, the two-centre term $T(1,2)$ can be approximated as

$$T(1,2) = \sum_{i\,\mathrm{m.o.}} C_i^* C_i / R_{12} = \sum_i q_i / R_{12}. \quad \text{(A 20)}$$

References

Abragam, A. & Bleaney, B. 1970 *Electron paramagnetic resonance of transition ions*. Oxford: Clarendon Press.

Allen, J. D. Jr., Boggess, G. W., Goodman, T. D., Wachtel, A. S. Jr. & Schweitzer, G. K. 1973 *J. electron. Spectrosc.* **2**, 289.

Baer, Y., Busch, G. & Cohn, P. 1975 *Rev. scient. Instrum.* **46**, 466.

Bakke, A. M. W. 1972 *J. molec. Spectrosc.* **41**, 1.

Bancroft, G. M. 1971 *Chem. Phys. Lett.* **10**, 449.

Bancroft, G. M., Adams, I., Creber, D. K., Eastman, D. E. & Gudat, W. 1976 *Chem. Phys. Lett.* **38**, 83.

Bancroft, G. M., Coatsworth, L. L., Creber, D. K. & Tse, J. S. 1977*a* *Physica Scr.* **16**, 217.
Bancroft, G. M., Coatsworth, L. L., Creber, D. K. & Tse, J. S. 1977*b* *Chem. Phys. Lett.* **50**, 228.
Bancroft, G. M., Creber, D. K. & Basch, H. 1977*c* *J. chem. Phys.* **67**, 4891.
Bancroft, G. M., Creber, D. K., Ratner, M. A., Moskowitz, J. W. & Topiol, S. 1977*d* *Chem. Phys. Lett.* **50**, 233.
Bancroft, G. M., Gudat, W. & Eastman, D. E. 1977*e* *J. electron. Spectrosc.* **10**, 407.
Bancroft, G. M. & Gutpa, R. P. 1978 *Chem. Phys. Lett.* **54**, 226.
Bancroft, G. M., Kumar Das, V. G. & Butler, K. D. 1974 *J. chem. Soc. Dalton, Trans.* 2355.
Bancroft, G. M., Malmquist, P. Å., Svensson, S., Basilier, E., Gelius, U. & Siegbahn, K. 1978 *Inorg. Chem.* **17**, 1595.
Bancroft, G. M. & Platt, R. H. 1972 *Adv. inorg. Chem. Radiochem.* **15**, 59.
Bancroft, G. M. & Sham, T. K. 1977 *J. magn. Reson.* **25**, 83.
Bancroft, G. M., Sham, T. K. & Larsson, S. 1977*f* *Chem. Phys. Lett.* **46**, 551.
Basch, H., Moskowitz, J. W., Hollister, C. & Hankin, D. 1971 *J. chem. Phys.* **55**, 1922.
Berkowitz, J. 1972 *J. chem. Phys.* **56**, 2766.
Berkowitz, J., Dehmer, J. L. & Walker, T. E. H. 1973 *J. chem. Phys.* **59**, 3645.
Berkowitz, J., Dehmer, J. L. & Walker, T. E. H. 1974 *J. electron. Spectrosc.* **3**, 323.
Boggess, G. W., Allen Jr., J. D. & Schweitzer, G. K. 1973 *J. electron. Spectrosc.* **2**, 467.
Brown, F. C., Bachrach, R. Z., Hagstrom, S. B. M., Lien, N. & Pruett, C. H. 1974 *Vacuum ultraviolet radiation physics* (ed. E. E. Koch), p. 785 and references. Oxford: Pergamon.
Carlson, T. A. 1975 *Photoelectron and Auger spectroscopy*, and references. New York and London: Plenum Press.
Comes, F. R., Haensel, R., Nielsen, U. & Schwartz, W. H. E. 1973 *J. chem. Phys.* **58**, 516.
Cornfield, A. B., Frost, D. C., MacDowell, C. A., Ragle, J. L. & Stenhouse, I. A. 1971 *J. chem. Phys.* **54**, 2651.
Dewar, M. J. S. 1969 *The molecular orbital theory of organic chemistry*. New York: McGraw Hill.
Eland, J. H. D. 1970 *Int. J. Mass Spectrom. Ion Phys.* **4**, 37.
Fischer, C. F. 1978 *Comp. Phys. Commun.* **14**, 145.
Gähwiller, Ch. & Brown, F. C. 1970 *Phys. Rev.* B2, 1918.
Gelius, U. 1974 *J. electron. Spectrosc.* **5**, 985.
Gelius, U., Basilier, E., Svensson, S., Bergmark, T. & Siegbahn, K. 1974*a* *J. electron. Spectrosc.* **2**, 405.
Gelius, U., Svensson, S., Siegbahn, H., Baslier, E., Faxlav, Å. & Siegbahn, K. 1974*b* *Chem. Phys. Lett.* **28**, 1.
Goodman, T. D., Allen, Jr., J. D., Cusachs, L. C. & Schweitzer, G. E. 1973 *J. electron. Spectrosc.* **3**, 289.
Gupta, R. P., Rao, B. D. & Sen, S. K. 1971 *Phys. Rev.* A **3**, 545.
Gupta, R. P. & Sen, S. K. 1973*a* *Electron Emission spectroscopy* (eds. W. Dekeyser *et al.*), p. 225: Holland, Reidel.
Gupta, R. P. & Sen, S. K. 1973*b* *Phys. Rev.* A **7**, 850.
Gupta, R. P. & Sen, S. K. 1973*c* *Phys. Rev.* A **8**, 1169, and references.
Gupta, R. P. & Sen, S. K. 1974 *Phys. Rev.* B **10**, 71.
Gupta, R. P., Tse, J. S. & Bancroft, G. M. 1978 *J. chem. Phys.* **68**, 4192.
Haas, H. & Shirley, D. A. 1973 *J. chem. Phys.* **58**, 3339.
Honig, A., Mandel, M., Stich, M. L. & Townes, C. H. 1954 *Phys. Rev.* **96**, 629.
Jones, P. G., Maddock, A. G., Mays, M. J., Muir, M. M. & Williams, A. F. 1977 *J. chem. Soc. Dalton Trans.* 1434.
Lindau, I., Pianetta, P., Yu, K. & Spicer, W. E. 1975 *Phys. Lett.* A **54**, 47.
Lücken, E. A. C. 1969 *Nuclear quadrupole coupling constants*, p. 93. New York: Academic Press.
McGuire, E. J. 1972 *Phys. Rev.* A **5**, 1043.
McGuire, E. J. 1974 *Phys. Rev.* A **9**, 1840.
McGuire, E. J. 1976 *Phys. Rev.* A **13**, 131, 1288.
Moore, C. E. 1971 *Natn. Bur. Stand.* (*U.S.*) Circ. no. 467.
Orchard, A. F. & Richardson, N. V. 1975 *J. electron. Spectrosc.* **6**, 61.
Perlow, G. J. 1968 *Chemical applications of Mössbauer spectroscopy* (ed. V. Goldanski & R. J. Herber), p. 377. New York: Academic Press.
Potts, A. W. & Price, W. C. 1977 *Physica Scr.* **16**, 191.
Potts, A. W. & Williams, T. A. 1977 *J. chem. Soc. Faraday Trans.* I, 1892.
Price, W. C., Potts, A. W. & Williams, T. A. 1974 *Proc. R. Soc. Lond.* A **341**, 147.
Rätner, M. A., Moskowitz, J. W. & Topiol, S. 1977 *Chem. Phys. Lett.* **46**, 495.
Schläfer, H. L. & Gliemann, G. 1969 *Basic principles of ligand field Theory*. New York: Wiley–Interscience.
Sevier, K. D. 1972 *Low energy electron spectrometry*. New York: Wiley–Interscience.
Sherwood, P. M. A. & Shirley, D. A. 1978 *Chem. Phys. Lett.* **56**, 404.
Slater, J. C. 1960 *Quantum theory of atomic structure*, vol. I. New York: McGraw Hill.
Shirley, D. A. 1973 *Adv. chem. Phys.* p. 85.
Siegbahn, K. *et al.* 1967 *ESCA-atomic molecular and solid state structure by means of electron spectroscopy*, ser. IV, vol. 20. Nova Acta Regiae Soc. Sci., Upaliensis, Uppsala, Sweden.
Siegbahn, K. *et al.* 1969 *ESCA applied to free molecules*. Amsterdam: North Holland.
Sternheimer, R. M. 1950 *Phys. Rev.* **80**, 102.
Sternheimer, R. M. 1966 *Phys. Rev.* **146**, 140.
Stevens, J. G. & Stevens, V. E. 1971 *Mössbauer effect data index*. New York: Plenum Press.

PHILOSOPHICAL TRANSACTIONS OF THE ROYAL SOCIETY A MATHEMATICAL, PHYSICAL & ENGINEERING SCIENCES

Stevens, K. W. H. 1952 *Proc. phys. Soc.* A **65**, 209.
Sutton, L. E. 1958 *Tables of interatomic distances and configuration in molecules and ions*. spec. publ. no. 2. London: The Chemical Society.
Sutton, L. E. 1965 *Tables of interatomic distances and configuration in molecules and ions*. spec. publ. no. 18. London: The Chemical Society.
Svensson, S., Mortensson, N., Basilier, E., Malmquist, P. Å., Gelius, U. & Siebgahn, K. 1976 *Physica Scr.* **14**, 141.
Turner, D. W., Baker, A. D., Baker, C. & Brundle, C. R. 1970 *Molecular photoelectron spectroscopy*. New York: John Wiley & Sons.
Veal, B. W. & Lam, D. J. 1974 *Phys. Rev. B* **10**, 4902.
Veal, B. W., Lam, D. J., Carnall, W. T. & Hoekstra, H. R. 1975 *Phys. Rev.* B **12**, 5651.
Vonbacho, P. S., Saltsburg, H., Ceasar, O. P. & Fleet, J. 1976 *J. electron. Spectrosc.* **8**, 359.
Wertheim, G. K. & Hüfner, S. 1973 *Phys. Rev. Lett.* **35**, 53.

PHILOSOPHICAL TRANSACTIONS OF THE ROYAL SOCIETY A MATHEMATICAL, PHYSICAL & ENGINEERING SCIENCES